The Plant Cell, Vol. 23: 4507–4525, December 2011, www.plantcell.org 

# GLYCOALKALOID METABOLISM1 Is Required for Steroidal Alkaloid Glycosylation and Prevention of Phytotoxicity in Tomato [W]

**Maxim Itkin,[a,1] Ilana Rogachev,[a] Noam Alkan,[b,2] Tally Rosenberg,[c] Sergey Malitsky,[a] Laura Masini,[d] Sagit Meir,[a] Yoko Iijima,[e,3] Koh Aoki,[e] Ric de Vos,[d] Dov Prusky,[b] Saul Burdman,[c] Jules Beekwilder,[d] and Asaph Aharoni[a,4]**

[a] Department of Plant Sciences, Weizmann Institute of Science, Rehovot 76100, Israel
[b] Agricultural Research Organization, The Volcani Center, Bet Dagan 50250, Israel
[c] Department of Plant Pathology and Microbiology, The Robert H. Smith Faculty of Agriculture, Food, and Environment, The Hebrew University of Jerusalem, Rehovot 76100, Israel
[d] Plant Research International, Wageningen 6700 AA, The Netherlands
[e] Kazusa DNA Research Institute, Kisarazu 292-0818, Japan

**Steroidal alkaloids (SAs) are triterpene-derived specialized metabolites found in members of the *Solanaceae* family that provide plants with a chemical barrier against a broad range of pathogens. Their biosynthesis involves the action of glycosyltransferases to form steroidal glycoalkaloids (SGAs). To elucidate the metabolism of SGAs in the *Solanaceae* family, we examined the tomato (*Solanum lycopersicum*) *GLYCOALKALOID METABOLISM1* (*GAME1*) gene. Our findings imply that GAME1 is a galactosyltransferase, largely performing glycosylation of the aglycone tomatidine, resulting in SGA production in green tissues. Downregulation of *GAME1* resulted in an almost 50% reduction in $\alpha$-tomatine levels (the major SGA in tomato) and a large increase in its precursors (i.e., tomatidenol and tomatidine). Surprisingly, *GAME1*-silenced plants displayed growth retardation and severe morphological phenotypes that we suggest occur as a result of altered membrane sterol levels caused by the accumulation of the aglycone tomatidine. Together, these findings highlight the role of GAME1 in the glycosylation of SAs and in reducing the toxicity of SA metabolites to the plant cell.**

## INTRODUCTION

The steroidal alkaloids (SAs), also known as solanum alkaloids, are common constituents of numerous plants belonging to the *Solanaceae* family, in particular members of the genus *Solanum* (Rahman et al., 1998), which comprises 1350 species. SAs have been extensively investigated for their diverse biological activities and occurrence in important crop plants (e.g., tomato [*Solanum lycopersicum*], potato [*Solanum tuberosum*], and eggplant [*Solanum melongena*]) (Eich, 2008). The synthesis of SAs, which is presumed to start from cholesterol, likely occurs in the cytosol and in most cases involves further glycosylation of the alkamine steroidal skeleton (aglycone) at C-3$\beta$ to form steroidal glycoalkaloids (SGAs) (Bowles, 2002; Friedman, 2002; Arnqvist et al., 2003; Kalinowska et al., 2005; Bowles et al., 2006).

In plants, SAs serve as phytoanticipins, providing the plant with a preexisting chemical barrier against a broad range of pathogens (Chan and Tam, 1985; Gunther et al., 1997; Sandrock and Vanetten, 1998; Hoagland, 2009). For example, tomato $\alpha$-tomatine acts via disruption of membranes, followed by the leakage of electrolytes and depolarization of the membrane potential (McKee, 1959; Steel and Drysdale, 1988; Keukens et al., 1992, 1995). However, it was suggested that tomato plants are not affected by its presence, possibly due the existence of sterol glycosides and acetylated sterol glycosides in tomato cell membranes (Roddick, 1976a; Steel and Drysdale, 1988; Blankemeyer et al., 1997). Glycosylation of SAs is believed to reduce the toxicity of $\alpha$-tomatine to the plant cell, as treatment of leaf disks from four plant species demonstrated that $\alpha$-tomatine caused more severe electrolyte leakage than did its aglycone tomatidine (Hoagland, 2009). In addition, studies of triterpene saponins in oat (*Avena sativa*) and *Medicago truncatula* pointed to the same role of glycosylation (Mylona et al., 2008; Naoumkina et al., 2010).

Recently, >50 different SAs were putatively identified in tuber extracts from seven genotypes (both wild and cultivated species) (Shakya and Navarre, 2008). In cultivated potato, $\alpha$-chaconine and $\alpha$-solanine comprise >90% of the total SAs. Three genes, encoding putative glycosyltransferases (GTs) involved in the biosynthesis of $\alpha$-solanine and $\alpha$-chaconine from the aglycone solanidine, have been identified in potato. The *Solanum tuberosum sterol alkaloid glycosyltransferase1* (*SGT1*) gene behaves in vitro as a UDP-Gal:solanidine galactosyltransferase (Moehs

[1] Current address: Agricultural Research Organization, The Volcani Center, PO Box 6, Bet Dagan 50250, Israel.
[2] Current address: Department of Plant Sciences, Weizmann Institute of Science, PO Box 26, Rehovot 76100, Israel.
[3] Current address: Faculty of Applied Bioscience, Kanagawa Institute of Technology, 1030 Shimo-ogino, Atsugi, Kanagawa 243-0292, Japan.
[4] Address correspondence to asaph.aharoni@weizmann.ac.il.
The author responsible for distribution of materials integral to the findings presented in this article in accordance with the policy described in the Instructions for Authors (www.plantcell.org) is: Asaph Aharoni (asaph.aharoni@weizmann.ac.il).
[W] Online version contains Web-only data.
www.plantcell.org/cgi/doi/10.1105/tpc.111.088732

et al., 1997). Silencing *SGT1* in potato resulted in redirection of the metabolic flux, causing strong reduction in accumulation of $\alpha$-solanine and significant accumulation of $\alpha$-chaconine, in which the primary glycosyl unit is Gal and Glc, respectively (McCue et al., 2005). *SGT2* was shown to encode a UDP-Glc:solanidine glucosyltransferase (McCue et al., 2006), which could mediate $\alpha$-chaconine biosynthesis. Finally, *SGT3* encodes a UDP-Rha: $\beta$-solanine/$\beta$-chaconine rhamnosyltransferase (McCue et al., 2007).

Approximately 100 different SAs have been described in various tomato tissues, particularly in fruit (Moco et al., 2006; Iijima et al., 2008; Kozukue et al., 2008; Mintz-Oron et al., 2008; Yamanaka et al., 2008). The major SA in tomato, $\alpha$-tomatine, was reported to be present in the green tissues of the plant together with dehydrotomatine (Kozukue et al., 2004). Whereas $\alpha$-tomatine levels decrease as the fruit matures and ripens, recent studies suggest a ripening-dependent conversion of $\alpha$-tomatine into esculeoside A, the most abundant SA in the red-ripe (RR) tomato fruit (Fujiwara et al., 2004; Moco et al., 2007; Iijima et al., 2008; Mintz-Oron et al., 2008; Yamanaka et al., 2009). The levels of esculeoside A appear to be ripening and ethylene dependent (Iijima et al., 2009). In tomato, very little is known about the enzymes and genes contributing to SA biosynthesis. A soluble protein fraction from tomato leaves was found to exhibit galactosyltransferase activity and weak glucosyltransferase activity (Zimowski, 1998). However, no experiments have been reported about genes that are relevant to SA content and play a role in tomato.

Here, identification of the *GLYCOALKALOID METABOLISM1* (*GAME1*) gene provides insight into the SA biosynthetic pathway in tomato. Glycosylation by GAME1 appears to be crucial to prevent the toxic effect of SAs to the plant cell, and GAME1 is likely involved in attaching the Gal group to the C-3$\beta$ position of tomatidine as part of the lycotetraose moiety formation. When *GAME1* is silenced, the new composition of SAs results in toxicity to the plant cell (most likely due to the increased levels of the aglycone tomatidine) and as a consequence causes marked developmental defects, including growth retardation. Our results suggest that this toxicity is due to alteration in sterol metabolism. We envisage that this work will promote future research to unravel further the SA pathway and its significance to plant fitness.

## RESULTS

### Metabolic Profiling Reveals Unique Clusters of SAs That Are Distributed across Diverse Tomato Plant Tissues

To examine the occurrence of SAs in different tomato (cv MicroTom) plant parts, we identified and examined the distribution of 85 putative SAs in 21 tissues and fruit developmental stages by ultraperformance liquid chromatography coupled to quadrupole time-of-flight mass spectrometry (UPLC-qTOF-MS) analysis (Figure 1; see Supplemental Table 1 online). Among the set of identified SAs, 47 represented those with a unique chemical formula, while the remaining substances were putatively identified as their isomers (see Supplemental Table 1 online). Hierarchical clustering of the profiling data revealed several clusters of tissue-/developmental stage–specific SAs. For example, 25 metabolites, including $\alpha$-tomatine, were associated with green tissues, as they were detected in unripe fruit, leaves, buds, and flowers (both containing sepals). We also detected 32 SAs associated with tissues of the RR fruit stage (in peel, flesh, and seeds). The levels of SAs were very low in pollen, consisting of only one SA (hydroxy-dehydrotomatidine trihexoside plus deoxyhexose), which was also found in pollen-containing buds and flowers. Apart from the 32 SAs unique to the RR fruit stage tissues, seeds harvested at that stage contained nine unique SAs. In roots, we identified two unique isomers of dehydrotomatine. Buds and flowers accumulated 14 SAs that were unique to these tissues, including five isomers of hydroxytomatine. The alkamine tomatidine, the precursor of $\alpha$-tomatine, was found at very low levels in most green tissues and in roots.

### GAME1 Is Part of a Clade of SA and Steroidal Saponin GTs

GTs of the plant Group 1 multigene family (120 members in *Arabidopsis thaliana*; Paquette et al., 2003) transfer the sugar moiety from UDP-sugar to a vast array of low molecular mass acceptors, including secondary metabolites and hormones (Bowles, 2002). As glycosylation of SAs is thought be crucial for their biological activity (Morrissey and Osbourn, 1999), we set out to discover tomato GTs that could act in the SA pathway. We used the nucleic acid sequence of the GT reported to glycosylate SAs in potato (St-*SGT1*; McCue et al., 2005) and identified three similar GTs from tomato (GAME1 to 3). In a phylogenetic analysis based on the publicly available full-length GT amino acid sequences (see Supplemental Figure 1 and Supplemental Data Set 1 online), these three tomato proteins formed a separate clade with GTs from potato (St-SGT1-3) that use SAs and two *Solanum aculeatissimum* proteins (Sa-GT4A and Sa-GT4R) shown to use both SAs and steroidal saponins as sugar acceptors (Moehs et al., 1997; Kohara et al., 2005; McCue et al., 2005, 2006, 2007). In this clade, the three GAME proteins each clustered most closely with one of the potato SGT proteins. Tomato *GAME1* (Sl-*GT1*; UGT73L5, according to the nomenclature guidelines; Mackenzie et al., 1997) exhibits 91% identity at the amino acid level to St-SGT1 (a UDP-Gal solanidine galactosyltransferase). Two additional tomato genes homologous to St-*SGT2* (coding for UDP-Glc:solanidine glucosyltransferase) and to St-*SGT3* (coding for UDP-Rha:$\beta$-solanine/$\beta$-chaconine rhamnosyltransferase) were named *GAME3* (UGT73L6) and *GAME2* (UGT73L4), respectively (see Supplemental Figure 1 and Supplemental Table 2 online). Further searches in genomic DNA scaffolds and comparison of the results with available BAC sequences (http://solgenomics.net) revealed that *GAME1* is located on chromosome 7.

### *GAME1* Expression Is Negatively Regulated by Ethylene during Fruit Ripening and Is Predominant in Green Tissues

We subsequently focused our interest on *GAME1* since its expression pattern was similar to the profile of SAs accumulating specifically in green tissues, being found primarily in young and mature leaves, peel, flesh, and seeds derived from immature and

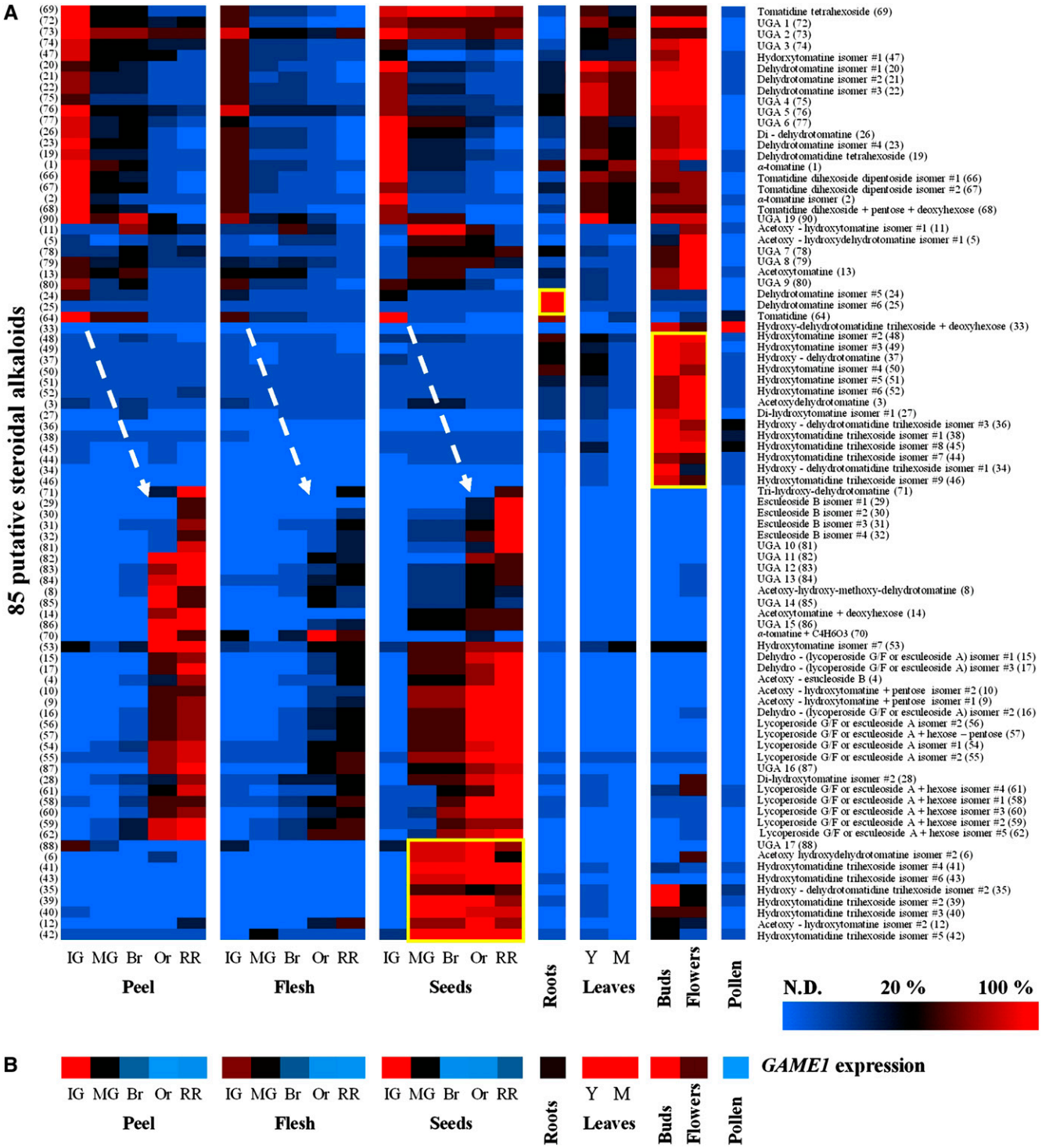


**Figure 1.** Diversity of SAs in Tomato and Its Correspondence with *GAME1* Expression.

**(A)** Diversity of SAs in tomato. Hierarchical clustering of SAs obtained by UPLC-qTOF-MS analysis. Yellow frames enclose several metabolite clusters discussed in the text, whereas white arrows indicate the possible conversion of green tissue–associated metabolites into RR tissue–associated metabolites during fruit ripening. Numbers within parentheses correspond to SAs in Supplemental Table 1 online. Relative levels of five additional putative SAs that were identified in the course of this study could not be measured. These substances are listed in Supplemental Table 1 online.

**(B)** *GAME1* expression in tomato tissues, measured by quantitative real-time PCR. The statistical significance of the gene expression data for each

mature green (MG) fruit and flower buds (Figures 1 and 2A). The tight association between *GAME1* transcript level and the accumulation of particular SAs, primarily $\alpha$-tomatine and dehydrotomatine isomers and derivatives in most of the examined tissues, suggested that it could be involved in the metabolism of this set of SAs. *GAME1* expression appeared to be downregulated during fruit ripening (Figure 2A). We further measured *GAME1* expression in fruit treated with 1-methylcyclopropene (1-MCP), an inhibitor of ethylene perception that negatively affects fruit ripening (Yokotani et al., 2009), finding that *GAME1* expression is negatively regulated by the ethylene signaling cascade that typically triggers the fruit ripening process (Figure 2B). *GAME1* expression was further examined in fruit of the *ripening inhibitor* (*rin*) and *non-ripening* (*nor*) mutants, which are also impaired in the ethylene signaling cascade (Herner and Sink, 1973; Thompson et al., 1999). *GAME1* transcript levels were significantly higher in the *nor* orange (Or) and RR fruit stages and in the *rin* RR stage (albeit a trend of increase was observed also at the Or stage; Figure 2C). Furthermore, *GAME1* expression seemed to be more affected in the *nor* background than in the *rin* mutant.

### Functional Characterization of the GAME1 Recombinant Enzyme Produced in *Escherichia coli* Cells and in Vivo Activity

The correlation between *GAME1* expression patterns and contents of $\alpha$-tomatine and its derivatives across the 21 different tomato plant tissues suggested that the enzyme it encodes might be acting in the formation of the $\alpha$-tomatine lycotetraose glycosyl chain. In $\alpha$-tomatine, this moiety contains two molecules of D-Glc and one each of D-Xyl and D-Gal, the latter attached to the tomatidine aglycone (see Supplemental Figure 2 online). We analyzed the specificity of GAME1 by in vitro enzyme assays using a recombinant enzyme produced in *E. coli*. UDP-Glc and UDP-Gal were compared as sugar donors with tomatidine as a substrate. UDP-Gal was readily used as a donor, producing a novel product with a mass-to-charge ratio of 578 *m/z* ([M+H]), corresponding to galactosylated tomatidine (Figure 3). Dehydrotomatidine (414 *m/z*; Figure 3), identified in the tomatidine standard as a contaminant (Kozukue et al., 2004), was also galactosylated by GAME1 (product 576 *m/z*). UDP-Glc was also incorporated to some extent, however, not exceeding 5% of the Gal incorporation under identical concentrations and conditions. This suggests that GAME1 is primarily a galactosyltransferase. The $K_m$ of GAME1 for tomatidine (in the presence of 8 mM UDP-Gal) was determined to be 38 $\pm$ 12 $\mu$M and the $k_{cat}$ 1.8 $\pm$ 0.4 $min^{-1}$. From these values, the catalytic efficiency ($k_{cat}/K_m$) was calculated as 783 $M^{-1}\cdot s^{-1}$. All other substrates tested showed lower catalytic efficiency or no turnover at all. In particular, solanidine and demissidine showed lower turnover rates, whereas solasonine was still in the same range of catalytic efficiency as tomatidine (see Supplemental Table 3 online). Apparently, the double bond between carbon 5 and carbon 6 in the B-ring of the solanidine and demissidine molecules interferes with efficient galactosylation. Other steroid substrates tested (cholesterol, campesterol, $\beta$-sistostanol, $\beta$-sitosterol, 24-epibrassinolide, and 24-epicastasterone) did not show any detectable product formation in the presence of GAME1 and UDP-Gal. Thus, GAME1 likely acts as a UDP-Gal galactosyltransferase for SAs, with a preference for tomatidine as a substrate.

We further examined tomatidine-galactosyltransferase activity in five tissues and developmental stages of wild-type plants (Figure 2D). The activity was consistent with *GAME1* expression levels as measured in these tissues, showing high levels in immature green peel and leaves (0.10 and 0.36 nmol·mg dry weight$^{-1}\cdot min^{-1}$, respectively) and relatively low activity in the RR peel and in roots (0.007 and 0.031 nmol·mg dry weight$^{-1}\cdot min^{-1}$, respectively).

### *GAME1*-Silenced Plants Display Severe Developmental Defects

To clarify the role of GAME1 in SA biosynthesis, we generated 18 independent transgenic tomato plants (in cv MicroTom) wherein *GAME1* was silenced via RNA interference (RNAi) using the *35S* cauliflower mosaic virus promoter (hereafter referred to as GAME1i plants). Interestingly, *GAME1* silencing had a strong effect on tomato plant growth and development, which is unexpected when silencing a gene associated with specialized metabolism. Seven GAME1i lines exhibited a severe phenotype (SPh) with strongly retarded growth compared with wild-type plants (Figure 4). These plants developed deformed leaves and produced numerous small flower buds that in most cases aborted before fertilization (Figures 4B to 4D and 4F). The low amount of fruit that occasionally developed in the SPh GAME1i plants was parthenocarpic and shriveled (Figure 4K). Four additional GAME1i plants exhibited a mild phenotype (MPh). These plants displayed normal plant architecture except for their fruit, which developed woody, possibly suberized regions, mostly around the fruit apex (Figures 4I and 4J). We further investigated one SPh and two MPh *GAME1* lines. *GAME1* transcript levels in GAME1i leaves were significantly reduced (see Supplemental Figure 3 online). At the enzymatic level, the tomatidine-galactosyltransferase activity was determined in mature leaf extracts derived from the GAME1i (SPh) line, constituting only 11% of the activity in the wild type (0.002 and 0.018 nmol·mg fresh weight$^{-1}\cdot min^{-1}$, respectively) (Figure 5A). Thus, silencing of *GAME1* resulted in a severe reduction in *GAME1* expression and reduced tomatidine-galactosyltransferase activity in the leaves.

The *GAME1i* construct was also introduced into the *Ailsa Craig* background, a typical indeterminate cultivar (see Supplemental

**Figure 1.** (continued).

examined tissue is presented in Figure 2A.

For **(A)** and **(B)**, the color index refers to the relative levels of a particular metabolite or the *GAME1* transcript across the different tissues examined; the highest level is defined as 100% ($n$ = 3). Br, breaker; IG, immature green; M, mature (fully expanded); Y, young.

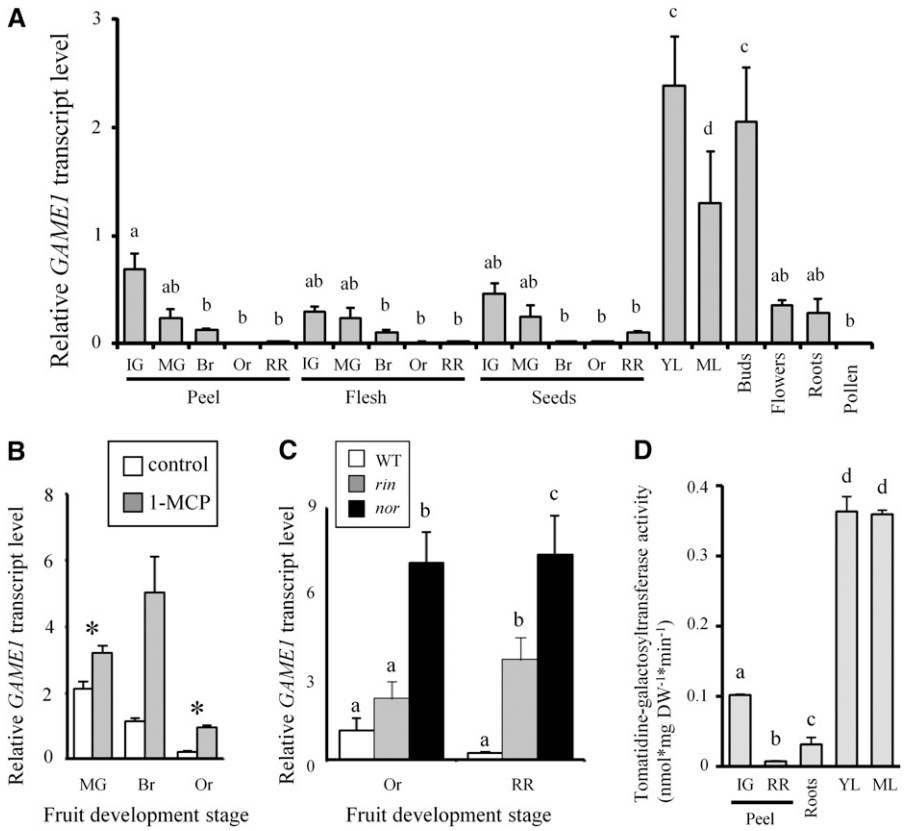


**Figure 2.** Expression of *GAME1* in the Wild Type and Fruit of the *rin* and *nor* Mutants and Tomatidine-Galactosyltransferase Activity in Wild-Type Tomato Tissues.

**(A)** Quantitative real-time PCR relative expression analyses of *GAME1* transcripts in 21 tissues of wild-type tomato (cv MicroTom). Different lettering above the bars denotes significant differences in gene expression as calculated by a Student's *t* test ($P < 0.05$; $n = 3$).

**(B)** *GAME1* expression is elevated in 1-MCP–treated fruit (cv Ailsa Craig) in the MG and Or developmental stages compared with untreated control fruit. Student's *t* test results for significance ($P < 0.05$; $n = 3$) are indicated by an asterisk.

**(C)** *GAME1* expression in tomato fruit of the *rin* and *nor* ripening mutants (cv Ailsa Craig) is higher than in fruit of the wild-type (WT) plants at the Or and RR fruit stages. Different lettering above the bars denotes significant differences in *GAME1* relative expression levels as calculated by a Student's *t* test ($P < 0.05$; $n = 3$).

**(D)** Tomatidine-galactosyltransferase activity in five tissues of tomato (cv MicroTom). Activity was measured in freeze-dried samples and is expressed on a dry weight (DW) basis. Different lettering above the bars denotes significant differences in activity as calculated by a Student's *t* test ($P < 0.05$; $n = 3$).

In all panels, the bars represent SE. Br, breaker; IG, immature green; ML, mature (fully expanded) leaves; YL, young leaves.

Figure 4 online). These plants were also deformed with strongly retarded growth (see Supplemental Figure 4B online) and displayed browning and suberized regions along the stem (Figure 4L; see Supplemental Figure 4C online). Although the Ailsa Craig GAME1i plants produced several flowers, they failed to bear fruit.

### Leaves of *GAME1*-Silenced Plants Exhibit Altered Levels of SAs

Metabolic profiling of SAs using UPLC-qTOF-MS was performed on extracts from GAME1i and wild-type leaves. Principal component analysis (PCA) indicated clear differences between the SA composition of extracts derived from SPh GAME1i leaves and those of the wild type (see Supplemental Figure 5A online). The SPh GAME1i leaf extracts contained significantly reduced levels of $\alpha$-tomatine and its isomer, three isomers of dehydrotomatine, hydroxy-dehydrotomatine, isomer #7 of hydroxytomatine, acetoxy-dehydrotomatine, dehydrotomatine tetrahexoside, and the unidentified glycoalkaloid (UGA) 4. On the other hand, hydroxytomatine isomer #4, acetoxy-hydroxytomatine isomer #1, and UGA 5 levels were increased approximately twofold in SPh GAME1i leaves relative to the wild type (Table 1; see Supplemental Figure 6 and Supplemental Table 4 online). In addition, we observed strong and significant accumulation of the $\alpha$-tomatine precursors: tomatidine and dehydrotomatidine (also named tomatidenol).

$\alpha$-Tomatine and tomatidine concentrations were measured in GAME1i and wild-type leaves. Interestingly, $\alpha$-tomatine levels were reduced more than 1.6-fold in SPh GAME1i compared with the wild type (Figure 5B). Moreover, the tomatidine aglycone was

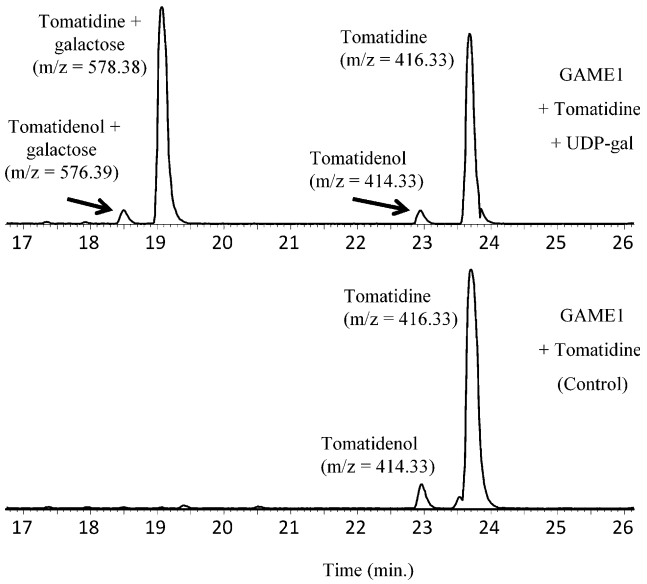


**Figure 3.** The Recombinant GAME1 Catalyzes the Galactosylation of Tomatidine.

Enzyme activity assays of the recombinant GAME1 produced in *E. coli* cells. The chromatograms (total ion count in UPLC-qTOF-MS) display analysis of the GAME1 recombinant protein incubated for 1 h with 0.25 mM tomatidine in the presence (top) or absence (bottom) of 8 mM UDP-Gal (UDP-gal). The *m/z* of eluting compounds is indicated. Arrows point to tomatidenol (dehydrotomatidine) (right) and dehydrotomatine plus Gal (left).

dramatically increased, from near baseline levels in wild-type leaves up to 290-fold in SPh GAME1i (Figure 5B). In the MPh GAME1i leaves, we observed an almost 1.6-fold reduction of $\alpha$-tomatine relative to the wild type (see Supplemental Figure 5C online). However, tomatidine and dehydrotomatidine levels in MPh GAME1i leaves were not different from the basal levels detected in wild-type leaves.

### MG Fruit of GAME1i Plants Display Altered Levels of SAs

SA profiles of MG fruit of the MPh GAME1i lines were compared with wild-type fruits using PCA (see Supplemental Figure 5B online). GAME1i plants with a severe phenotype were excluded from this analysis, as they produced very few fruit. Profiles of MG fruit from MPh GAME1i were clearly different from the wild type (see Supplemental Figure 5B online). In MG fruit of the GAME1i #1 and GAME1i #2 lines, we measured a reduction in numerous green tissue–associated SAs, including $\alpha$-tomatine, and in hydroxy-dehydrotomatidine trihexoside plus deoxyhexose, whereas elevated levels were recorded for tomatidine (5 times more than in wild-type MG fruit) and its isomer, isomer #4 of lycoperoside G/F or esculeoside A plus hexose, several hydroxytomatine isomers, $\alpha$-tomatine plus C4H6O3, and UGA 9 (Figure 6). A detailed description of SAs that were altered in the GAME1i fruit tissues is presented in Table 1, Figure 6, and Supplemental Table 4 online.

A proposed pathway that represents the biosynthesis and metabolism of SAs during tomato fruit development (from the immature green to the RR stage) was generated based on previously published data (Friedman, 2002; Kozukue et al., 2004; Moco et al., 2007; Iijima et al., 2008, 2009; Mintz-Oron et al., 2008) and the data from this study (Figure 6).

### *GAME1*-Silenced Plants Exhibit Altered Sterol Composition

As the severe developmental phenotype observed in the SPh GAME1i plants was similar to phenotypes of brassinosteroid or gibberellic acid ($GA_3$) biosynthesis and signaling mutants (Bishop et al., 1999; Ueguchi-Tanaka et al., 2005), we attempted to restore the GAME1i phenotype by application of 24-epibrassinolide, 24-epicastasterone, or $GA_3$. Although application of $GA_3$ restored the internode elongation of SPh GAME1i plants to some extent, treatments with both brassinosteroid substances were ineffective (data not shown).

Alteration of sterol metabolism was also considered as a reason for the morphological changes, since SA and sterol biosynthesis are tightly linked (Arnqvist et al., 2003). Moreover, tomatidine, which accumulates to high levels in GAME1i plants, was reported to mimic the effect of sterol biosynthesis inhibitors (Simons et al., 2006). Therefore, the concentrations of 10 different sterols and triterpenoids were measured via gas chromatography (GC)–MS analysis of leaves from SPh GAME1i, a set of segregating F1 plants that displayed a normal wild-type phenotype, and the wild type. Major differences were observed in the composition of sterols and triterpenoids, both in pathway intermediates as well as in end products, particularly in the two branches downstream of 24-methylenelophenol (Figure 7A; see Supplemental Figure 7 online). Whereas campesterol levels increased 1.8-fold, the levels of stigmasterol and its precursor $\beta$-sitosterol were reduced. Small but significant reductions in cycloartenol and $\beta$-amyrin were measured in SPh GAME1i leaves. Interestingly, $\alpha$-amyrin, (*S*)-2,3-oxidosqualene, cholesterol, lanosterol, and cholestanol were detected at their native levels. Segregating F1 plants bearing a wild-type phenotype had a sterol profile comparable to that of the wild type (see Supplemental Figure 7 online). The GAME1i phenotype could not be rescued by application of $\beta$-sitosterol, stigmasterol, or both (data not shown).

Misbalanced phytosterol levels in the *Arabidopsis cycloartenol synthase* mutant result in bleaching of inflorescence shoots and chloroplasts lacking the thylakoid membrane system and starch granules and accumulating large plastoglobuli-like vesicles (Babiychuk et al., 2008). Although no bleaching was observed in GAME1i plants, transmission electron microscopy (TEM) revealed major changes in plastid ultrastructure. Chloroplasts of SPh GAME1i leaves possessed large plastoglobuli (0.4 $\mu$m in diameter compared with 0.2 $\mu$m in wild-type plants) and altered starch grain and grana structures (Figures 7B to 7E).

### Stress Response–Related Symptoms and Gene Expression in *GAME1*-Silenced Plants

We introduced the *GAME1i* construct into the indeterminate M82 cultivar by crossing, obtaining plants that displayed a phenotype resembling that of the cv MicroTom and cv Ailsa Craig GAME1i lines, including severe growth retardation, deformed leaves, and abortion of flower buds (see Supplemental Figures 8A and 8B


**Figure 4.** *GAME1*-Silenced Tomato Plants Display Severe Morphological Phenotypes.

**(A)** and **(B)** Three-week-old (3w) wild-type (WT) and GAME1i (SPh) tomato plants (cv MicroTom), respectively.
**(C)** and **(D)** Six-week-old (6w) GAME1i SPh tomato plants (cv MicroTom).
**(E)** and **(F)** Four-month-old (4m) wild-type and GAME1i (SPh) tomato plants (cv MicroTom), respectively.
**(G)** to **(K)** MG and RR wild-type tomato fruit (cv MicroTom; **[G]** and **[H]**) compared with fruit in the corresponding stages of the MPh GAME1i plants [**(I)** and **(J)**] and to the SPh GAME1i RR stage fruit **(K)**.
**(L)** Suberized stem of a GAME1i plant (cv Ailsa Craig).

online). In addition, leaves of these plants exhibited dark necrotic spots resembling symptoms typically seen after infection of tomato by pathogenic bacteria like *Xanthamonas campestris* pv *vesicatoria* (*Xcv*) or *Pseudomonas syringae* pv *tomato* (see Supplemental Figures 8C and 8D online; Jones et al., 1991). As no other tomato lines grown in the same greenhouse at the same time showed similar disease-like symptoms, we hypothesized that silencing *GAME1* might mimic induction of disease symptoms in the absence of a pathogen. Indeed, we were not able to isolate *Xcv* or *P. syringae* pv *tomato* (or other putative pathogens) from GAME1i leaves that displayed necrotic spots.

Microarray analysis was performed to examine if the transgene, and possibly, the corresponding changes in the metabolic profile, induced the plant response system at the transcriptional level. Eleven and 24 genes showed significant down- and upregulated expression, respectively, in GAME1i leaves (see Supplemental Table 5 online). The set of upregulated transcripts was enriched (eight in total, ~33%) in genes that are upregulated in response to bacterial attack (*ENOLASE* [Gibly et al., 2004], two *GDSL LIPASE* homologs [Hong et al., 2008], and *ETHYLENE-RESPONSIVE PROTEINASE INHIBITOR1* [Pautot et al., 1991]) as well as to other pathogens (*CARBOXYESTERASE* [Ko et al., 2005], *ISOCITRATE DEHYDROGENASE* [*ICDH*] [Jang et al., 2003], *PR5-LIKE PROTEIN/NP24* [Rodrigo et al., 1991], and *PEROXIDASE* [*PER*] [Vera et al., 1993]) (see Supplemental Table 5 online). To verify the microarray results, we performed quantitative real-time PCR, which showed that the expression of seven out of 10 examined genes was indeed significantly altered (see Supplemental Figure 8E online). These included five genes that were upregulated in *GAME1*-silenced plants (*PER*, *ENOLASE*, *PR5-LIKE*, *DICYANIN*, and *GDSL LIPASE*) and two genes (*HAT22-LIKE* and *CLAVAMINATE SYNTHASE-LIKE*) that were downregulated. These results support a significant alteration in expression of multiple biotic stress–related genes in the SPh GAME1i plants.

### Extracts of *GAME1*-Silenced Plants and Tomatidine Itself Inhibit *Arabidopsis* Root Growth

As described above, the metabolic composition of *GAME1*-silenced plants had a strong effect on tomato plant growth and development. We tested whether this toxicity affects growth and

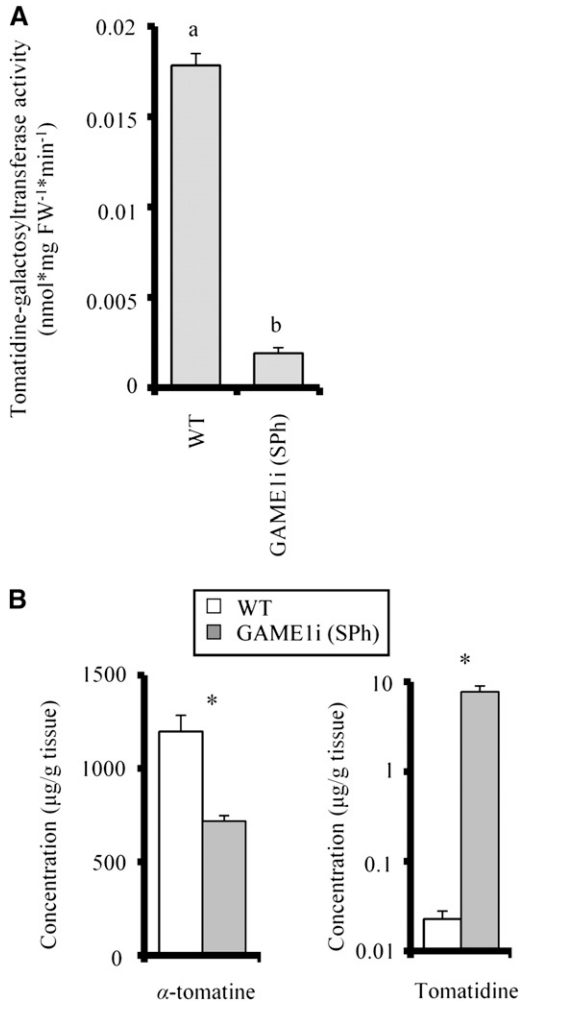


**Figure 5.** Altering *GAME1* Expression Has a Major Effect on in Planta Tomatidine-Galactosyltransferase Activity and on Levels of $\alpha$-Tomatine and Tomatidine.

**(A)** Tomatidine-galactosyltransferase activity in fully expanded leaves (cv MicroTom, 4-week-old plants). Activity was measured in extracts derived from fresh samples and is expressed on a fresh weight (FW) basis. Different lettering above the bars denotes significant differences in tomatidine-galactosyltransferase activity levels as calculated by a Student's *t* test ($P < 0.05$; $n = 3$). WT, wild type.

**(B)** GAME1i plants exhibit reduced levels of $\alpha$-tomatine and accumulation of its precursor tomatidine. Their absolute concentrations were measured in fully expanded leaves of the wild type (4-week-old plants) and compared with those of SPh GAME1i plants of similar age (using UPLC-qTOF-MS). Significant differences according to a Student's *t* test ($P < 0.05$; $n = 3$) are indicated by an asterisk.

In **(A)** and **(B)**, the bars represent SE.

development of other plant species as well. No differences in germination rate or frequency were observed between *Arabidopsis* seeds sown on plates containing leaf extracts from wild-type or GAME1i plants. However, SPh GAME1i extracts showed a major effect on *Arabidopsis* root growth; after 3 weeks, roots of seedlings on medium containing SPh GAME1i extracts were 50% shorter than those on medium with wild-type extracts (see Supplemental Figures 9A, 9B, and 9E online).

To examine the possible cytotoxic role of $\alpha$-tomatine and tomatidine, *Arabidopsis* seeds were germinated on media supplemented with range of $\alpha$-tomatine or tomatidine concentrations. No difference in germination rate or frequency was observed, but there was significant root growth retardation that was positively correlated with tomatidine levels at concentrations above 0.003 $\mu$g per mL medium (see Supplemental Figures 9C and 9D online). By contrast, there was no correlation between root length and the amount of supplemented $\alpha$-tomatine (see Supplemental Figure 9D online). When 1-week-old tomato seedlings were sprayed with various concentrations of tomatidine for 3 weeks, they did not exhibit a similar phenotype.

### An Altered SA Profile Impacts Pathogenicity and Growth of Tomato Disease Agents

Several fungi and bacteria possess tomatinases that cleave the lycotetraose chain at various positions of $\alpha$-tomatine (Sandrock and Vanetten, 1998; Morrissey and Osbourn, 1999; Kaup et al., 2005). Given our finding that *GAME1* silencing affects expression of biotic stress–related genes, we examined whether altered SA glycosylation levels impact pathogenicity or growth of several tomato disease agents. SPh and MPh GAME1i leaf extracts inhibited germination and growth of the pathogenic fungi *C. coccodes* to a lesser extent than did wild-type leaf extracts (see Supplemental Figures 10A to 10C online). In addition, SPh GAME1i extracts gave rise to decreased halo inhibition compared with MPh GAME1i extracts (see Supplemental Figures 10A and 10C online). The effect of *GAME1* silencing on plant susceptibility to the bacterial pathogen *Xcv* was evaluated in inoculation experiments, revealing altered bacterial growth in GAME1i leaves compared with the wild-type (see Supplemental Figure 11 online).

## DISCUSSION

In this study, we identified GAME1, a GT-type enzyme that uses UDP-Gal to attach the first sugar moiety to the alkamine tomatidine. This discovery not only provides important insight into the SGA biosynthetic pathway in tomato but also sheds light on the significance of glycosylation in the prevention of self-toxicity in plants.

### Negative Regulation of *GAME1* Expression and Green Tissue–Related SAs by Climacteric Ethylene Signaling during Tomato Fruit Development

Metabolic profiling assays performed in recent years have revealed a plethora of SAs in tomato and potato, beyond those reported earlier in these two species (Moco et al., 2006; Iijima et al., 2008; Kozukue et al., 2008; Mintz-Oron et al., 2008; Shakya and Navarre, 2008). The examination of almost 90 different SAs in this study highlights this remarkable diversity, while describing several groups of related chemicals that cluster together across the 21 different tomato tissues and organs studied. One notable cluster, largely represented by $\alpha$-tomatine and dehydrotomatine

**Table 1.** SAs Altered in the *GAME1* RNAi Tomato Lines

| | | | Downregulated | | Upregulated | |
|---|---|---|---|---|---|---|
| No. | Putative Metabolite | *m/z* (+) | Leaf | Fruit (MG) | Leaf | Fruit (MG) |
| 1 | $\alpha$-Tomatine | 1034.5536 | + | + | | |
| 2 | $\alpha$-Tomatine isomer | 1034.5564 | + | + | | |
| 3 | Acetoxy-dehydrotomatine | 1090.5434 | + | | | |
| 11 | Acetoxy-hydroxytomatine isomer #1 | 1108.5540 | | | + | |
| 18 | Dehydrotomatine (tomatidenol) | 414.3500 | + | | | |
| 19 | Dehydrotomatidine tetrahexoside | 1062.5485 | + | | | |
| 20 | Dehydrotomatine isomer #1 | 1032.5379 | + | + | | |
| 21 | Dehydrotomatine isomer #2 | 1032.5379 | + | + | | |
| 22 | Dehydrotomatine isomer #3 | 1032.5379 | + | + | | |
| 23 | Dehydrotomatine isomer #4 | 1032.5379 | | + | | |
| 24 | Dehydrotomatine isomer #5 | 1032.5379 | | + | | |
| 26 | Didehydrotomatine | 1030.5223 | | + | | |
| 33 | Hydroxy-dehydrotomatidine trihexoside + deoxyhexose | 1062.5485 | | + | | |
| 37 | Hydroxy-dehydrotomatine | 1048.5327 | + | | | |
| 48 | Hydroxytomatine isomer #2 | 1050.5485 | | | | + |
| 49 | Hydroxytomatine isomer #3 | 1050.5485 | | | | + |
| 50 | Hydroxytomatine isomer #4 | 1050.5585 | | | + | |
| 51 | Hydroxytomatine isomer #5 | 1050.5485 | | | | + |
| 53 | Hydroxytomatine isomer #7 | 1050.5585 | + | | | |
| 61 | Lycoperoside G/F or esculeoside A + hexose isomer #4 | 1432.6596 | + | | | + |
| 64 | Tomatidine | 416.3529 | | | + | + |
| 65 | Tomatidine isomer | 416.3529 | | | | + |
| 66 | Tomatidine dihexoside dipentoside isomer #1 | 1004.5430 | | + | | |
| 69 | Tomatidine tetrahexoside | 1064.5641 | | + | | |
| 70 | $\alpha$-Tomatine + C4H6O3 | 1136.5861 | | | | + |
| 75 | UGA 4 | 1044.5379 | + | | | |
| 76 | UGA 5 | 1046.5536 | | | + | |
| 77 | UGA 6 | 1052.5620 | | + | | |
| 80 | UGA 9 | 1122.5696 | | | | + |

A "+" indicates a significant change in at least one transgenic line; no "+" indicates a nonsignificant change.

derivatives, is present in green tomato tissues, including buds and flowers (containing green sepals). Interestingly, this cluster showed a similar pattern in fruit peel, flesh, and seeds, suggesting a common regulatory network for coordinated SA metabolism in the different fruit tissues. Such a mechanism could be climacteric ripening, which typically brings about a myriad of metabolic changes in the fruit during the transition from immature green to RR fruit. However, while most studies on climacteric ripening focus on the pericarp tissue, these results tie together ripening and secondary metabolism in the peel and seeds as well. The link between the temporal and spatial production of SAs in tomato and the ripening process is even more significant in light of the increased production of $\alpha$-tomatine in *rin*, *nor*, and *Never-ripe* (*Nr*) mutants and the decrease in $\alpha$-tomatine content in ethylene-treated fruit reported by Iijima et al. (2009). In agreement with these findings, we also found increased *GAME1* expression in 1-MCP–treated fruit as well as in fruit of *rin* and *nor* mutants. Transcriptional regulation related to fruit maturation has been investigated extensively; however, most of these studies focused on genes that are upregulated during fruit maturation and ripening (Rose et al., 1997; Bartley and Ishida, 2003; Itkin et al., 2009; Karlova et al., 2011). By contrast, *GAME1* exhibits downregulated expression during the course of fruit maturation and is negatively regulated by climacteric ethylene signaling. It is expected that genes encoding enzymes catalyzing acetylation or glycosylation steps downstream in the $\alpha$-tomatine catabolism pathway will be positively regulated by ripening and the ethylene cascade.

A second cluster of SAs represents metabolites of tomatine that accumulate at the later Or and RR stages of fruit development and are mainly represented by lycoperoside G/F or esculeoside A derivatives. Again, these display a similar pattern in flesh, peel, and seed tissues. Apart from the presence of green SAs that are produced in the sepals, a unique set of hydroxytomatine and its derivatives is present in buds and flowers. The cluster of esculeoside A and its derivatives typically produced in fruit during the ripening process (see above) could not be detected in these tissues. This latter observation suggests that floral organs lack enzyme activity for conversion of hydroxylated SAs to esculeoside A and its isomers and derivatives.

### GAME1 Acts Predominantly as a UDP-Gal: Tomatidine Galactosyltransferase

The promiscuity of members of the GT superfamily to which GAME1 belongs and the possibility that in vitro assays with a recombinant enzyme do not reflect native, in planta activities complicates the functional characterization of such enzymes.

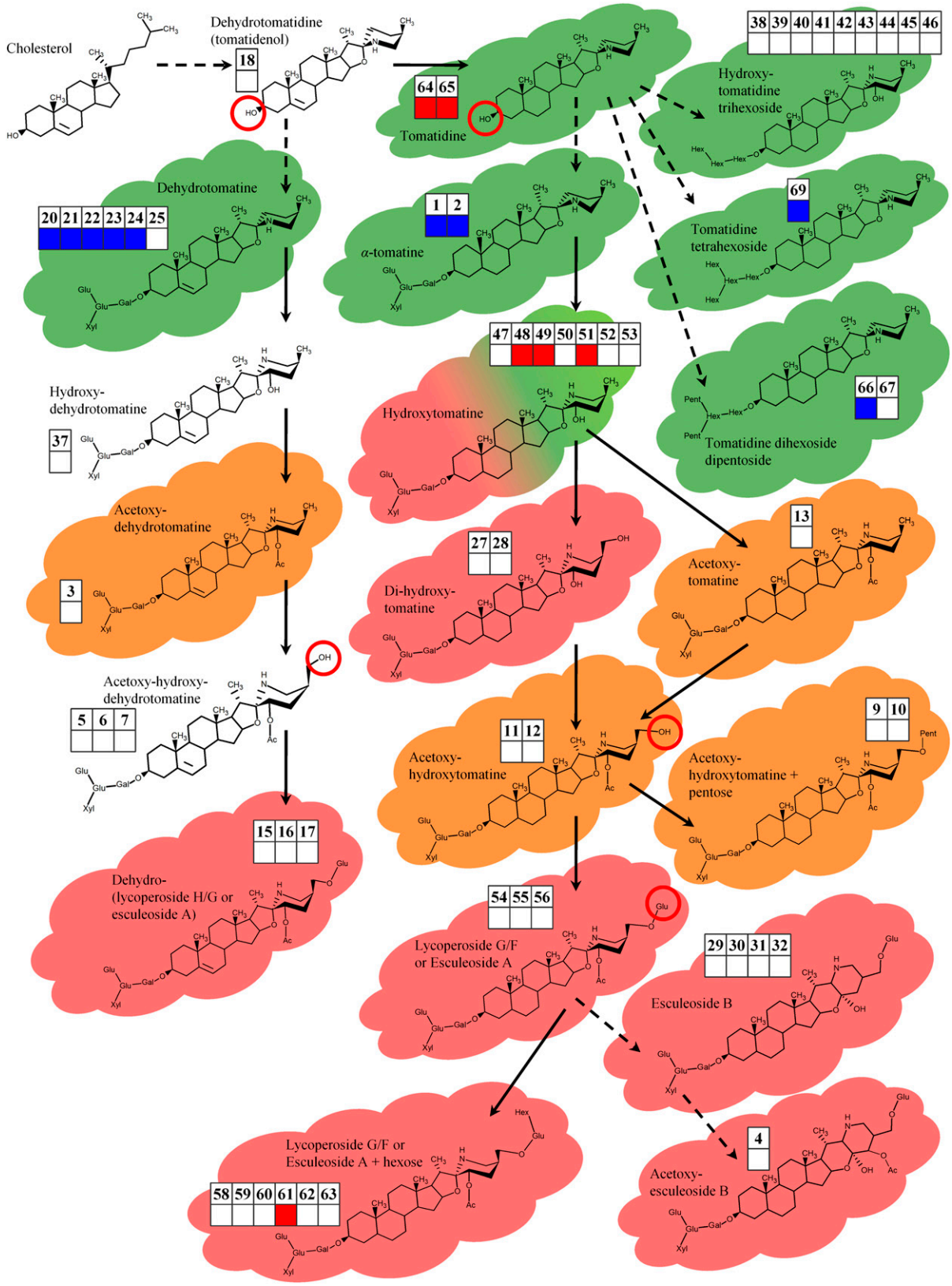


**Figure 6.** Changes to SA Levels in MG Fruit of *GAME1*-Silenced Plants.

Nevertheless, we provide strong evidence that tomato *GAME1* encodes a UDP-Gal:tomatidine galactosyltransferase. The similarity of GAME1 to other reported SA and saponin GTs from related *Solanaceae* plant species, particularly potato SGT1 reported to act as a UDP-Gal:solanidine galactosyltransferase, provides evidence for the putative function of GAME1.

Recombinant enzyme activity assays showed that the *GAME1*-encoded enzyme catalyzes the transfer of Gal to the tomatidine aglycone with high efficiency and the transfer of Glc to a lesser extent. The putative green tissue–associated SA catabolism pathway contains three additional steps in which acetoxy-hydroxy-dehydrotomatine, acetoxy-hydroxytomatine, and esculeoside A (or lycoperoside G/F) are glycosylated. However, recombinant GAME1 was not active with the latter two substrates (data not shown). As *GAME1* expression is reduced after the MG fruit stage and the glycosylated products of the three predicted additional glycosylation reactions occur only later in fruit development, it is likely that GAME1 catalyzes the early glycosylation reaction with tomatidine as a substrate. Moreover, the role of GAME1 in galactosylation of tomatidine is supported by the colinearity of gene expression and enzyme activity in tomato tissues and the strong reduction in tomatidine-galactosyltransferase activity in *GAME1*-silenced lines.

In potato, the ratio of 3-*O*-glycosylated SAs is coordinated by two solanidine-modifying enzymes, SGT1 and SGT2, which catalyze the galactosylation and glucosylation of solanidine, respectively (Moehs et al., 1997; McCue et al., 2005), and is determined by relative expression of the corresponding genes (*SGT1* and *SGT2*) within tissues (McCue et al., 2005, 2006). In most cultivated potato species, derivatives of 3-O-glucosylsolanidine are more abundant than those of 3-*O*-galactosylsolanidine (Friedman et al., 2003). Interestingly, several genotypes of *Solanum chacoense* exhibit higher relative levels of *SGT1* (galactosyltransferase) than of *SGT2* (glucosyltransferase), suggesting an opposite SA 3-*O*-glycosylation ratio (galactosylation/glucosylation) (Krits et al., 2007). Enzyme activity assays performed herein, together with previously published data (Zimowski, 1998), support a different mechanism in tomato for regulating the 3-*O*-glycosylated SA ratio. We suggest that this ratio is largely determined by the substrate specificity of the GAME1 enzyme, capable of producing 3-*O*-galactosyltomatidine and to some extent 3-*O*-glucosyltomatidine. In this case, 3-*O*-glucosyltomatidine derivatives probably constitute only a minor fraction of the numerous SA isomers in tomato.

Metabolic profiling of MG stage fruit from *GAME1*-silenced lines provided evidence that GAME1 is essential for the formation of the lycotetraose moiety of tomatidine and dehydrotomatidine aglycones through attachment of a Gal moiety. Silencing of *GAME1*-reduced glycosylation of tomatidine and dehydrotomatidine, which could be observed as a decrease in $\alpha$-tomatine, dehydrotomatine, tomatidine conjugated to four hexose moities, and tomatidine with two hexose and two pentose moieties, all of these products likely being glycosylated through the action of GAME1. In leaves, the predicted activity of GAME1 in glycosylation of tomatidine and dehydrotomatidine was further corroborated by the SA profile of *GAME1*-silenced lines. There was a dramatic decrease in $\alpha$-tomatine levels, a corresponding accumulation of its aglycone tomatidine and of tomatidine's precursor dehydrotomatidine and up to a 90% reduction in dehydrotomatine. Assays with recombinant GAME1 further supported that it acts on dehydrotomatidine, since the commercial tomatidine standard likely contained dehydrotomatidine; therefore, GAME1 used dehydrotomatidine as substrate as well as tomatidine (Kozukue et al., 2004; Figure 3, peaks lacking two protons [*m/z* = 414] next to the main peaks).

Unexpectedly, in both MG fruits and leaves of *GAME1*-silenced lines, we observed accumulation of intermediates that are downstream of $\alpha$-tomatine (Figure 6; see Supplemental Figure 6 online). This suggests that feed-forward, posttranscriptional mechanisms might be activated in RNAi lines in which *GAME1* expression is only partially silenced. Alternatively, it is possible that the downstream portion of the current $\alpha$-tomatine metabolic pathway model is incomplete. The inability of tomato to reroute the excess tomatidine accumulating in SPh *GAME1*-silenced plants provides us with the opportunity to investigate the role of glycosylation of SAs in vivo. Such study could not be done in potato, in which silenced *SGT1* does not lead to a strong phenotype, likely due to redirection of metabolic flux from solanidine toward $\alpha$-chaconine (McCue et al., 2005).

## Phytotoxicity Observed in *GAME1*-Silenced Plants and Their Raison d'Être

SAs including $\alpha$-tomatine and its corresponding aglycone, tomatidine, are toxic to a broad range of organisms, including bacteria, fungi, animals, and even plants themselves (Chan and Tam, 1985; Gunther et al., 1997; Sandrock and Vanetten, 1998; Pareja-Jaime et al., 2008; Hoagland, 2009).

**Figure 6.** (continued).

Metabolites that are abundant at the immature green and MG stages are marked with a green background, those abundant at the breaker and orange stages with an orange background, and those abundant at the RR stage are marked with a red background. Metabolites placed on a white background were not detected in fruit tissues. In the squares, elevated and reduced metabolite levels in fruit of *GAME1*-silenced plants are marked with red and blue colors, respectively, while a lack of color represents no change in metabolite levels. The numbering of the isomers of a particular metabolite is according to the putative SA numbers in Supplemental Table 1 online. Dashed arrows represent multiple biosynthetic reactions, solid arrows represent a single biosynthetic reaction, and possible points of glycosylation activity of GAME1 are encircled. Acetoxy-hydroxy-methoxy-dehydrotomatine (8), acetoxytomatine + deoxyhexose (14), dehydrotomatidine tetrahexoside (19), di-dehydrotomatine (26), hydroxy-dehydrotomatidine trihexoside + deoxyhexose (33), three isomers of hydroxy-dehydrotomatidine trihexoside (34, 35, and 36), lycoperoside G/F or esculeoside A + hexose - pentose (57), tomatidine dihexoside + pentose + deoxyhexose (68), $\alpha$-tomatine + C4H6O3 (70), and tri-hydroxy-dehydrotomatine (71) were not included in this scheme.

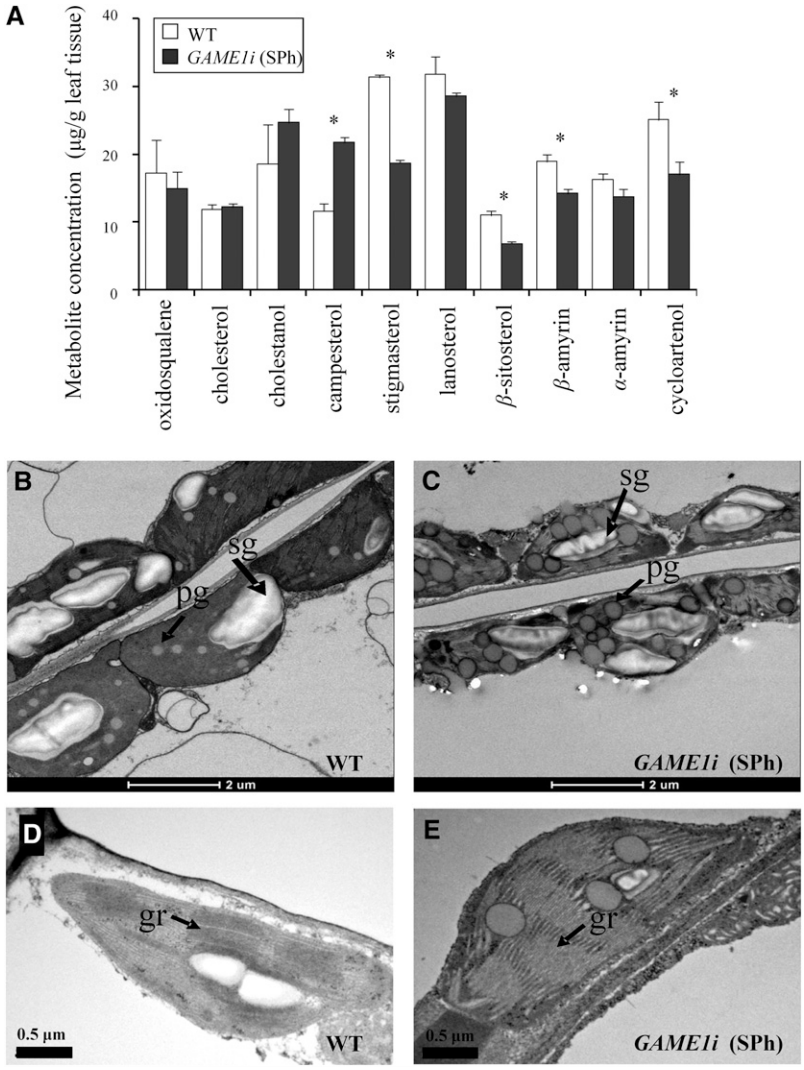


**Figure 7.** *GAME1*-Silenced Plants Are Altered in Their Sterol Profile and Plastid Morphology.

**(A)** Absolute concentrations of 10 detected phytosterols in fully expanded leaves of 4-week-old GAME1i plants compared with wild-type (WT) plants of a similar age were measured using GC-MS (see Methods). In **(A)**, the bars represent SE. Sterols that were found to be significantly altered by a Student's *t* test ($P < 0.05$; for the wild type, $n = 5$; for GAME1i, $n = 6$) are marked with an asterisk. The proposed pathway of sterol metabolism in plants and changes in leaves of *GAME1*-silenced plants are shown in Supplemental Figure 7B online.

**(B)** and **(D)** TEM images of plastids in cells of mature leaves of the wild-type. In **(B)**, starch grains (sg), plastoglobuli (pg), and grana (gr) are indicated with arrows.

**(C)** and **(E)** TEM images of plastids in cells of mature leaves of a SPh GAME1i plant.

Sterols are essential for normal plant growth and development, and they affect genes involved in cell division and cell expansion likely through a brassinosteroid-independent pathway. Therefore, altering their composition could result in dramatic developmental phenotypes (Carland et al., 2002, 2010; He et al., 2003). Whereas $\alpha$-tomatine damages tissues within an array of plant species (Hoagland, 2009), its toxic effects in tomato fruit and leaves were suggested to be negligible due to the presence in cell membranes of sterol glycosides and acetylated sterol glycosides rather than sterols such as cholesterol, containing a free 3$\beta$-OH group (with which $\alpha$-tomatine forms insoluble complexes) (Roddick, 1976a; Steel and Drysdale, 1988; Blankemeyer et al., 1997). Glycosylation of membrane steroids serves a protective function against toxic compounds, including saponins (Naoumkina et al., 2010). Incomplete glycosylation of the triterpene glycoside (i.e., saponin) avenacin results in degeneration of the epidermis and altered root hair development in oat (Mylona et al., 2008). Moreover, *M. truncatula* growth is severely affected by alterations in glycosylation of the saponin hederagenin (Naoumkina et al., 2010). More specifically for tomato SAs, Hoagland (2009) showed that tomatidine had a greater effect than $\alpha$-tomatine in electrolyte leakage tests performed on leaves of a number of plant species.

The severe growth retardation, altered plant architecture, and necrosis we observed in *GAME1*-silenced plants may have several explanations. Sugar donors UDP-Glc and/or UDP-Gal may accumulate, possibly resulting in synthesis of other glycosides or accumulation of other classes of chemicals as a result of a nonspecific stress response, as suggested by Naoumkina et al. (2010). *GAME1*-silenced plants that displayed a severe phenotype exhibited a dramatic increase in levels of the aglycone tomatidine compared with other transgenic lines that did not show visual phenotypes, including those with less efficient silencing of *GAME1* expression. Since tomatidine was previously shown to interfere with ergosterol biosynthesis in yeast (Simons et al., 2006), we examined the sterol profile of the *GAME1*-silenced plants and found it to be significantly altered compared with the wild type. Simons et al. (2006) reported a reduction in the levels of zymosterol, when yeast was grown on media supplemented with tomatidine, consistent with inhibition of C24 sterol methyltransferase Erg6p. Thus, a possible explanation for the unusual sterol profile in *GAME1*-silenced plants could be tomatidine-mediated inhibition of sterol methyltransferase 2 (SMT2), the plant Erg6p ortholog. As a result, $\beta$-sitosterol and stigmasterol levels would be reduced while 24-methylenelophenol was channeled toward campesterol. The altered sterol profile could be related to the damage in the leaf chloroplast ultrastructure, consistent with the accumulation of enlarged plastoglobuli and lack of organized thylakoid membrane structure and starch granules in the *Arabidopsis cycloartenol synthase1* mutant (Babiychuk et al., 2008). This is further supported by data showing that the campesterol to $\beta$-sitosterol ratio modulates *Arabidopsis* growth and is controlled by SMT2 (Schaeffer et al., 2001). In addition, the reduction in *Arabidopsis* root growth on media supplemented with tomatidine-containing extracts from GAME1i tomato plants is comparable with the finding that sterols downstream of *Arabidopsis* SMT2 and its homolog SMT3 are crucial for proper root development (Carland et al., 2010). Consistent with the inability of sterol treatment to complement plants defective in SMT2 (Carland et al., 2010), our attempts to reverse the GAME1i phenotype by application of $\beta$-sitosterol and/or stigmasterol were unsuccessful. The effect of *GAME1* silencing on sterol metabolism demonstrates once again the tight link between SAs and the sterol pathway (Arnqvist et al., 2003).

The distribution and compartmentalization of SAs within the plant cell is currently unclear; however, it was suggested that SGAs in potato and tomato are located in the soluble phase, most possibly in the vacuole, of the vegetative or fruit (tomato) cells (Roddick, 1976b, 1977). Therefore, we suggest that the glycosylation of hydrophobic alkamines leads to SA solubilization and plays a fundamental role in the protection of plant cells against the harmful compounds they produce.

### Alteration of SA Glycosylation Affects Fungal Growth

Similar to other defensive secondary metabolites, SAs are part of the coevolution between plants and pathogens (Morrissey and Osbourn, 1999; Arie et al., 2007). Several fungal and bacterial species possess tomatinases that are capable of removing part or even the entire lycotetraose structure from tomatine. By doing so, the toxicity of these substances toward the pathogens is reduced and the damage to the host plant may increase (Sandrock and Vanetten, 1998; Morrissey and Osbourn, 1999; Bouarab et al., 2002; Ito et al., 2004; Oka et al., 2006). Moreover, derivatives of $\alpha$-tomatine hydrolysis could also mediate suppression of plant defenses (Bouarab et al., 2002; Ito et al., 2004). $\alpha$-Tomatine is toxic to several fungi; thus, the reduced levels of $\alpha$-tomatine we observed in leaf extracts of *GAME1*-silenced plants may explain the reduced inhibition of germination and growth of the fungal pathogen *C. coccodes*.

## Conclusions

Here, we characterized one of three *GAME* genes that likely mediate the formation of the lycotetraose moiety of $\alpha$-tomatine, the major SA produced by tomato. The findings provide insight into SA metabolism in tomato and the role of SA glycosylation in plant growth and interaction with pathogens. Experiments are currently underway to investigate the function of *GAME2* and *GAME3* in tomato SA biosynthesis. The recently predicted pathway for $\alpha$-tomatine metabolism during fruit development suggests that additional GTs might take part in this process. Resolving the glycosylation steps and eventually the entire SA pathway at the molecular level should be a main target for future SA research. Current research in model plants of the *Solanaceae* will set the stage to expand our understanding of the evolution and metabolism of these specialized metabolites, for example, in the more complex monocot species of the *Liliaceae* family.

## METHODS

### Tomato Plant Material and Generation of Transgenic Tomato Plants

Tomato plants (*Solanum lycopersicum*) cv MicroTom, cv Ailsa Craig (obtained from the Tomato Genetics Resource Center; http://tgrc.ucdavis.edu), and cv M82 were grown in a climate-controlled greenhouse at 24°C during the day and 18°C during night, with natural light. Fruit was used at immature green, MG, breaker, Or, and RR stages and was picked on average 10, 35, 38, 41, and 44 d after anthesis, respectively. The *GAME1*-silenced construct (RNAi; *GAME1i*) was created by introducing the *GAME1* fragment to pENTR/D-TOPO (Invitrogen) (by *Asc*I and *Not*I) and further transfer of the *GAME1* fragment from the resulting plasmid to the pK7GWIWG2 (II) binary vector (Karimi et al., 2002) using Gateway LR Clonase II enzyme mix (Invitrogen). Primers used in this work are listed in Supplemental Table 6 online. Constructs were transformed into cv MicroTom and cv Ailsa Craig as described by Meissner et al. (1997, 2000). The introduction of *GAME1i* into cv M82 was done by crossing wild-type tomato cv M82 with transgenic tomato cv MicroTom carrying *GAME1i* and exhibiting SPh. As SPh GAME1i plants were unable to set seeds, they were crossed with wild-type cv MicroTom, and the segregating F1 plants exhibiting a severe phenotype were used in further experiments.

### Phylogenetic Analysis

Nucleic acid sequence of the potato (*Solanum tuberosum*) SGT1 (McCue et al., 2005) was used to search publically available databases: Dana Farber Cancer Institute Gene Indices (http://compbio.dfci.harvard.edu/tgi/), SOL (http://solgenomics.net/), MiBASE (http://www.pgb.kazusa.or.jp/mibase/), and the National Center for Biotechnology Information (http://blast.ncbi.nlm.nih.gov). Amino acid sequences of the five best hits in tomato, several identified plant GTs, and GTs with unknown or

putative function were aligned using ClustalX version 2 program (Larkin et al., 2007). The aligned sequences are shown in Supplemental Data Set 1 online. GenBank and tentative contig numbers are shown in the Supplemental Table 7 online. An unrooted phylogenetic tree was built using the SeaView v.4.2.5 program (Gouy et al., 2010) using the maximum likelihood method by PhyML 3.0 (Guindon and Gascuel, 2003) with the following settings: model, LG; branch support, aLRT (SH-like); invariable sites, optimized; across site rate variation, optimized; tree searching operations, best for Nearest Neighbor Interchanges and Subtree Pruning and Regrafting; starting tree, BioNJ, optimize tree topology.

### Preparation of Extracts

If not stated otherwise, tissues (200 mg) of tomato were frozen in liquid nitrogen and ground to a fine powder using an analytical mill (IKA; A11 basic) or mortar and pestle. Then, frozen tissue was extracted with 80% methanol:water (v/v) containing 0.1% formic acid (the solid:liquid ratio was kept at 1:3 [w/v]). The mixture was vortexed for 30 s, sonicated for 30 min at room temperature, vortexed again for 30 s, centrifuged (20,000*g*, 10 min), and filtered through a 0.22-μm polytetrafluoroethylene membrane filter (Acrodisc CR 13 mm; PALL).

### Targeted Profiling of Tomato Metabolites

The profiling of SAs in organic extracts of tomato tissues was performed by MS analyses, performed by the UPLC-qTOF instrument (Waters High Definition MS System; Synapt), with the UPLC column connected online to a photo diode array detector (Waters, Acquity), and then to the MS detector, equipped with an electrospray probe. Separation of metabolites and detection of the eluted compound masses was performed as described by Mintz-Oron et al. (2008) and Adato et al. (2009). Masses were detected in the *m/z* range of 50 to 1500 D with the following settings: capillary voltage at 3.0 kV, cone voltage at 28 eV, collision energy at 4 eV, and argon was used as a collision gas. For MS/MS, 10 to 60 eV were used (for both ionization modes). Tomatidine and α-tomatine were identified by comparison of their retention times and MS/MS fragments to those of the corresponding standard compounds. Their concentrations in planta were quantified against standards using standard curves. Dehydrotomatine and dehydrotomatidine were identified by comparison to the corresponding compounds present as impurities in standards (tomatidine [Sigma-Aldrich] and α-tomatine [Apin Chemicals]). Other metabolites were putatively identified as follows: The elemental composition, selected according to the accurate masses and the isotopic pattern using the MassLynx software, and MS/MS fragments were compared with those found in the literature (Cataldi et al., 2005; Moco et al., 2006; Iijima et al., 2008; Mintz-Oron et al., 2008; Yamanaka et al., 2008). Relative quantification of the compounds was performed with the QuanLynx program version 4.1 (Waters) using the data acquired in the positive mode. Peak areas were used for the hierarchical clustering of the SAs with MeV version 4.5.1 software (http://www.tm4.org/mev). Peak areas after *ln* transformation and quantile normalization inside each group of replicates were used for the construction of the PCA plots.

### Phytosterol Analysis

Phytosterol content of tomato was analyzed as described by the *Arabidopsis* Metabolomics Consortium (http://tht.vrac.iastate.edu:81/media/protocols/Analytical%20Platform_5.pdf) with slight modifications. Fully expanded tomato leaves were frozen in liquid nitrogen and ground to a fine powder using a mortar and pestle. Subsequently, 150 mg frozen leaf powder was extracted at 75°C for 60 min with 6 mL chloroform/methanol (2:1 [v/v]; containing 1.25 mg/L epicholesterol [Steraloids] as an internal standard). Extracts were kept at room temperature for at least 1 h, solvents were evaporated to dryness in the lyophilizer, and the remaining residue was saponified at 90°C for 60 min in 2 mL 6% (w/v) KOH in methanol. Upon cooling to room temperature, 1.5 mL *n*-hexane and 1.5 mL water were added, and the mixture was shaken vigorously for 20 s. Following centrifugation (3000*g* for 2 min) to separate the phases, the hexane phase was transferred to a 2-mL Eppendorf tube and evaporated to dryness using a gentle stream of nitrogen. The aqueous phase was reextracted with 1.5 mL *n*-hexane and centrifuged, and the hexane phase was added to a 2-mL Eppendorf tube containing the pellet from the first extraction and evaporated as above. Subsequently, 50 μL of *N*-methyl-*N*-trimethylsilyl trifluoroacetamide was added to the pellet, the sample was shaken vigorously for 30 s, and the mixture was transferred to a 2-mL autosampler glass vial with a 100-μL conical glass insert. After capping the vial, the reaction mixture was incubated at room temperature for at least 15 min. The GC-MS system comprised a COMBI PAL autosampler (CTC Analytics), a trace GC ultra-gas chromatograph equipped with a programmable temperature vaporizing (PTV) injector, and a DSQ quadrupole mass spectrometer (Thermo Electron). GC was performed on a 30 m × 0.25 mm × 0.25-μm Zebron ZB-5 ms MS column (Phenomenex). The PTV split technique was performed as follows: Samples were analyzed in the constant temperature splitless mode. PTV inlet temperature was set at 280°C. Analytes were separated using the following chromatographic conditions: Helium was used as carrier gas at a flow rate of 1.2 mL/min. The thermal gradient started at 170°C, was held at this temperature for 1.5 min, ramped to 280°C at 37°C/min and then ramped to 300°C at 1.5°C/min and held at 300°C for 5.0 min. Eluents were fragmented in the electron impact mode with an ionization voltage of 70 eV. The reconstructed ion chromatograms and mass spectra were evaluated using Xcalibur software version 1.4 (ThermoFinnigan). Compounds were identified by comparison of their retention index and mass spectrum to those generated for authentic standards analyzed on the same instrument: α-amyrin (Apin Chemicals); β-sitosterol, β-amyrin, cholestanol, cholesterol, and stigmasterol (Sigma-Aldrich); lanosterol, cycloartenol, and campesterol (Steraloids), and 2,3-oxidosqualene (Echelon Biosciences). Phytosterol concentrations in planta were quantified against standards using standard curves.

### Quantitative Real-Time PCR

RNA isolation from fruit (without placenta and seeds) was performed by the hot phenol method (Verwoerd et al., 1989) from seeds (cleaned from gel) as described by Ruuska and Ohlrogge (2001) and from all other tissues by the Trizol method (Sigma-Aldrich). DNase 1 (Sigma-Aldrich) treated RNA was reverse transcribed using a high-capacity cDNA reverse transcription kit (Applied Biosystems). Gene-specific oligonucleotides were designed by the Primer Express 2 software (Applied Biosystems). The *CLATHRIN ADAPTOR COMPLEXES* subunit gene (Expósito-Rodríguez et al., 2008) was used as an endogenous control. Additional primers used for quantitative real-time PCR are listed in Supplemental Table 6 online.

### Generation and Purification of GAME1 Recombinant Enzyme

*GAME1* was amplified from cDNA using oligonucleotides listed in Supplemental Table 6 online. The amplification product was subcloned into pACYCDUET-1 using *Bam*HI and *Pst*I restriction enzymes. The resulting plasmid, pAC-GAME1 (carrying the GAME1 open reading frame fused to N-terminal 6XHis tag), was transformed to *Escherichia coli* BL21 DE3 (Novagen, Merck). For expression of the GAME1 enzyme, a fresh overnight culture was diluted 1:100 in 25 mL 2× yeast-tryptone medium with 30 μg/mL chloramphenicol and incubated at 37°C and 250 rpm until an $OD_{600}$ of 0.4 was reached. Subsequently, isopropyl-β-D-thio-galactoside was added to a concentration of 0.5 mM, and the incubation continued overnight at 18°C and 250 rpm. The next day, cells were harvested by centrifugation and the pellet resuspended in 2 mL of 50 mM Tris HCl, pH 7.5, with 8 mM β-mercaptoethanol. After breaking the cells by sonication, insoluble material was removed by centrifugation, and the soluble fraction

was treated with Ni-nitrilotriacetic acid spin columns (Qiagen) according to the manufacturer's instructions for purification of the recombinant protein. The solution containing purified protein (200 μL) was dialyzed in the presence of 2 liters of 50 mM Tris HCl, pH 7.5,with 8 mM β-mercaptoethanol at 4°C. After addition of 15% (v/v) of glycerol, protein was stored at −20°C until further analysis. Protein concentration was determined using the Bio-Rad protein assay by comparison to a BSA standard.

### Enzyme Assays with GAME1 Recombinant Enzyme

The substrates tomatidine (Sigma-Aldrich), solanidine, solasodin, and demissidin (kindly supplied by Harry Jonker) as well as 23-acetoxy-27-hydroxytomatine and esculeoside A (kindly provided by Yoko Iijima and Koh Aoki) were all dissolved in 1 mM DMSO. Enzyme assays were performed in 50 mM Tris-HCl, pH = 7.5, with 8 mM β-mercaptoethanol using 5 μg/mL enzyme, 8 mM UDP-Gal or UDP-Glc, and 0.1 mM substrate (or, for determination of kinetic constants, 0.1 mM, 0.05 mM, 0.025 mM, 0.01 mM, and 5 μM) in a volume of 100 μL. After 1 h of incubation under slight agitation at 30°C, reactions were stopped by addition of 300 μL methanol and 0.1% formic acid. Samples were prepared by vortexing briefly and sonication for 15 min. Then, the extracts were centrifuged for 5 min at 20,000*g* and filtered through 0.2-μm inorganic membrane filters (RC4; Sartorius). The identification of products was performed using a Waters Alliance 2795 HPLC connected to a Waters 2996 photo diode array detector and subsequently a qTOF Ultima V4.00.00 mass spectrometer (Waters, MS Technologies) operating in the positive ionization mode. The column used was an analytical column (Luna 3 μ C18/2 100A; 2.0 × 150 mm; Phenomenex) attached to a C18 precolumn (2.0 × 4 mm; AJO-4286; Phenomenex). Degassed eluent A (ultrapure water:formic acid [1000:1, v/v]) and eluent B [acetonitrile:formic acid (1000:1, v/v]) were used at 0.19 mL/min. The gradient started at 5% B and increased linearly to 75% B in 45 min, after which the column was washed and equilibrated for 15 min before the next injection. The injection volume was 5 μL. The amount of substrate consumed was measured by the decrease in peak surface area in the LC-MS chromatogram, relative to a control from which UDP-Gal was omitted. Masses used were tomatidine ($C_{27}H_{45}NO_2$; 416.35 *m/z* ([M+H]), solanidine ($C_{27}H_{43}NO$; 398.34 *m/z* ([M+H]), solasodine ($C_{27}H_{43}NO_2$; 414.34 *m/z* ([M+H]), and demissidine ($C_{27}H_{45}NO$; 400.36). Kinetic constants were calculated using Lineweaver-Burk plots (Lineweaver and Burk, 1934).

### GAME1 Protein Activity

To test tomatidine-galactosyltransferase activity in tissues, freeze-dried material or fresh material was deep frozen, ground to a fine powder, and stored at −80°C. The powder (20 mg freeze-dried or 125 mg fresh) was extracted for 5 min at 4°C with 0.7 mL of a buffer consisting of 50 mM Tris-HCl, pH 8.0, 1 mM EDTA, 0.1% Triton X-100, 5 mM DTT, 3% polyvinylpolypyrrolidone, and Protease Inhibitor Mix P (Serva). Of the supernatant after centrifuging for 10 min at 13,000*g* and 4°C, 0.25 mL was collected and applied to a NAP-5 column (GE-Healthcare) equilibrated in 50 mM Tris-HCl, pH 8.0, 1 mM EDTA, 0.1% Triton X-100, and 2 mM DTT. The column was washed and eluted using 0.25 and 0.7 mL of the same buffer. Of this crude protein extract, 100 μL was used in the enzyme assay, in a final volume of 200 μL. Concentrations in the assay were 50 mM Tris-HCl, pH 8.0, 1 mM EDTA, 0.1% Triton X-100, 2 mM DTT, 10 mM UDP-Gal (Sigma-Aldrich), and 0.1 mM tomatidine. After 2 h of incubation under slight agitation at 30°C, reactions were stopped by addition of 600 μL methanol and 0.1% formic acid. Analysis was performed as described for the recombinant protein.

### Microarray Assays

Total RNA was extracted from three pools of the third to sixth true leaves in a single plant using TRIZOL (Sigma-Aldrich) and treated with DNase 1 (Sigma-Aldrich). Biotinylated cRNA was fragmented and hybridized to the Affymetrix GeneChip Tomato Genome Array as described in the Affymetrix technical manual (www.affymetrix.com). Statistical analysis of microarray data was performed using the Partek Genomics Suite (www.partek.com) and the robust microarray averaging algorithm (Irizarry et al., 2003). Changes in expression levels were determined by analysis of variance. False discovery rate was applied to correct for multiple comparisons (Benjamini and Hochberg, 1995). Differentially expressed genes were chosen according to false discovery rate < 0.1 and a twofold change between genotypes and signal above background in at least one microarray. Functional annotation analysis was performed manually using publicly available databases.

### Bacterial Strains and Inoculation Techniques

For inoculation, *Xcv* strain 97-2 (race T3; *X. perforans* according to the new nomenclature; Astua-Monge et al., 2000) was grown on nutrient agar (NA; Difco Laboratories) at 28°C for 48 h. Cells were resuspended in a solution containing 10 mM $MgCl_2$ with 0.02% Silwet L-77. Bacterial concentrations were adjusted using a spectrophotometer and verified by plating of serial dilutions on NA. Tomato plants were grown from seeds in a greenhouse (25 to 28°C) in 0.6-liter spots containing a mixture of equal parts of sand, vermiculite, and peat. Inoculation of plants for assessment of *Xcv* growth in planta was performed by vacuum dipping 7- to 8-week-old plants into bacterial suspensions of $5 \times 10^5$ colony-forming units/mL as described by Tamir-Ariel et al. (2007). Seven plants per treatment were inoculated in each experiment. To determine bacterial concentration in inoculated leaves, leaf discs were extracted from the first three fully expanded leaves, homogenized, serial diluted, and plated onto NA plates with cephalexin (25 μg/mL). This experiment was repeated three times.

### *Colletotrichum coccodes* Halo Inhibition Assay

Organic extracts from 660 or 200 mg wild-type and transgenic plant leaves were dried by nitrogen bubbling and dissolved in 200 μL of 70% methanol in water. The extracts (from 200 mg for spore germination assay and from 660 mg for growth inhibition assay) were loaded on 13-mm Whatman discs and air dried, then the discs were placed in the center of Petri dishes containing Mathur's medium (Tu, 1985), which were previously inoculated with $5 \times 10^5$ *C. coccodes* spores. The Petri dishes were incubated overnight at 4°C and then transferred to 27°C for assessment of fungal growth and germination. Twenty-four hours later, the growth inhibition haloes were measured and photographed.

### Application of Brassinosteroids, $GA_3$, β-Sitosterol, Stigmasterol, and 1-MCP Treatment

Plants were sprayed to the point of runoff with 24-epibrassinolide (1 μM), 24-epicastasterone (1 μM), $GA_3$ (100 ppm), or β-sitosterol (150 ppm) and/or stigmasterol (150 ppm) dissolved in water with addition of 0.5% ethanol and 0.02% Silwet L-77 for 2 weeks every 2 d. For 1-MCP treatment, fruits (cv Ailsa Craig) at the MG, breaker, and Or stages were incubated with 1 ppm of 1-MCP for 19 h, transferred to open air for 24 h, and subsequently frozen. Control fruits were incubated in air instead of 1-MCP.

### TEM

For TEM, fully expanded leaves from 6-week-old tomato plants were collected and processed using a standard protocol (Chuartzman et al., 2008). The Epon-embedded samples were sectioned (70 nm) using an ultramicrotome (Leica) and observed with a Technai T12 transmission electron microscope (FEI).

### *Arabidopsis thaliana* Root Inhibition Assay

*Arabidopsis* ecotype Columbia seeds were sown on Murashige and Skoog medium (Murashige and Skoog, 1962) supplemented with leaf extracts from wild-type or GAME1i plants (0.5 g tissue) or with various concentrations of $\alpha$-tomatine or tomatidine (all dissolved in DMSO, resulting in 0.5% of DMSO in medium). *Arabidopsis* germinated on Murashige and Skoog medium supplemented only with 0.5% DMSO was used as control. After imbibition of 48 h, Petri dishes with plants were transferred to the climate room (24°C, a 16/8-h light/dark cycle, $20 \pm 2$ $\mu E \cdot m^{-2} \cdot s^{-1}$).

### Accession Numbers

Sequence data from this article can be found in the GenBank/EMBL data libraries under accession numbers HQ293016, HQ293018, and HQ293017, for GAME1, GAME2, and GAME3, respectively. Additional accession numbers used in this article are listed in Supplemental Table 7 online. Microarray data are available in the ArrayExpress database (www.ebi.ac.uk/arrayexpress) under accession number E-MEXP-3455.

### Supplemental Data

The following materials are available in the online version of this article.

**Supplemental Figure 1.** A Separate Clade of Enzymes Acting on Steroidal Alkaloids and Steroidal Saponins in the Large Plant Glycosyltransferase Protein Family.

**Supplemental Figure 2.** Structures of Tomatidine and $\alpha$-Tomatine.

**Supplemental Figure 3.** Relative *GAME1* Transcript Levels in the Leaves of Transgenic Plants Used in This Study.

**Supplemental Figure 4.** Phenotypes of Tomato Plants with Altered Expression of *GAME1*.

**Supplemental Figure 5.** Altering *GAME1* Expression Has a Major Effect on Steroidal Alkaloid Metabolism.

**Supplemental Figure 6.** Changes to Steroidal Alkaloid Levels in Leaves and Fruit of *GAME1*-Silenced Plants.

**Supplemental Figure 7.** *GAME1*-Silenced Plants Are Altered in Their Sterol Profile.

**Supplemental Figure 8.** Silencing of GAME1 Results in Altered Expression of Stress- and Bacterial Response–Associated Genes.

**Supplemental Figure 9.** *Arabidopsis* Root Growth Is Inhibited by Supplementation of the Medium with Extracts Derived from GAME1i Plants or with Tomatidine but Not with $\alpha$-Tomatine.

**Supplemental Figure 10.** Growth and Spore Germination of the Fungus *Colletotrichum coccodes* Is Altered on Medium Containing Leaf Extracts of *GAME1*-Silenced Plants.

**Supplemental Figure 11.** Silencing of the *GAME1* Gene in Tomato Alters Tomato Susceptibility to the Bacterial Pathogen *Xanthomonas campestris* pv *vesicatoria*.

**Supplemental Table 1.** Putative Steroidal Alkaloids Identified in Tomato Tissues.

**Supplemental Table 2.** Sequence Comparison of GAME and SGT Orthologs from Potato and Tomato.

**Supplemental Table 3.** Structures and Turnover Percentage of Different Steroidal Alkaloids Mediated by the Recombinant GAME1 Enzyme.

**Supplemental Table 4.** Fold Changes in Steroidal Alkaloid Levels in Leaves or Fruit between GAME1i and the Wild Type.

**Supplemental Table 5.** Genes with Significantly Altered Expression in the Leaves of the GAME1i Plant.

**Supplemental Table 6.** Primers Used in This Study.

**Supplemental Table 7.** Accession Numbers of the Sequences Used for the Construction of the Phylogenetic Tree (Supplemental Figure 1 Online).

**Supplemental Data Set 1.** Alignment of Glycosyltransferase Sequences Used for the Generation of the Phylogenetic Tree.

## ACKNOWLEDGMENTS

We thank Danny Gamrasni for 1-MCP–treated fruits, Ester Feldmesser for assistance with array data analysis, Eyal Shimoni for TEM analysis, Leonid Brodsky for assistance with the PCA analysis, Oran Barkan for technical help with the experiments, Peter Mackenzie for assistance with naming *GAME* genes, and Arie Tishbee and Riri Kramer for operating the UPLC-qTOF-MS instrument. We also thank Louise Chappell-Maor for her careful and critical reading of our manuscript. J.B. acknowledges the EU 7th Frame ATHENA Project (FP7-KBBE-2009-3-245121-ATHENA) for financial support. R.d.V. acknowledges the Centre of Biosystems Genomics. The work of T.R. was supported by Grant 975/07 from the Israel Science Foundation. A.A. is the incumbent of the Adolpho and Evelyn Blum Career Development Chair of Cancer Research. Work in A.A.'s laboratory was supported by the Minerva Foundation and the European Research Council Project SAMIT (FP7 Program).

## AUTHOR CONTRIBUTIONS

M.I. designed and performed the research, analyzed metabolomics data, and wrote the article. I.R. assisted with metabolomics data analysis. N.A. performed the fungal assays and wrote the article. T.R. performed the bacterial assays. S. Malitsky assisted with the GC-MS metabolomics data analysis and operated the GC-MS. L.M. assisted with in vitro enzyme activity assays. S. Meir assisted with metabolomics data analysis. Y.I. purified metabolites for in vitro enzyme activity assays. K.A. purified metabolites for in vitro enzyme activity assays. R.d.V. analyzed the results of in vitro and in planta enzyme activity assays (LC-MS). D.P. assisted in fungal assays. S.B. assisted in bacterial assays and wrote the article. J.B. performed in vitro and in planta enzyme activity assays and wrote the article. A.A. designed the research and wrote the article.

Received July 1, 2011; revised November 6, 2011; accepted November 29, 2011; published December 16, 2011.

## REFERENCES

**Adato, A., et al.** (2009). Fruit-surface flavonoid accumulation in tomato is controlled by a SlMYB12-regulated transcriptional network. PLoS Genet. **5:** e1000777.

**Arie, T., Takahashi, H., Kodama, M., and Teraoka, T.** (2007). Tomato as a model plant for plant-pathogen interactions. Plant Biotech. **24:** 135–147.

**Arnqvist, L., Dutta, P.C., Jonsson, L., and Sitbon, F.** (2003). Reduction of cholesterol and glycoalkaloid levels in transgenic potato plants by overexpression of a type 1 sterol methyltransferase cDNA. Plant Physiol. **131:** 1792–1799.

**Astua-Monge, G., Minsavage, G.V., Stall, R.E., Davis, M.J., Bonas, U., and Jones, J.B.** (2000). Resistance of tomato and pepper to T3

strains of *Xanthomonas campestris* pv. *vesicatoria* is specified by a plant-inducible avirulence gene. Mol. Plant Microbe Interact. **13:** 911–921.

**Babiychuk, E., Bouvier-Navé, P., Compagnon, V., Suzuki, M., Muranaka, T., Van Montagu, M., Kushnir, S., and Schaller, H.** (2008). Allelic mutant series reveal distinct functions for Arabidopsis cycloartenol synthase 1 in cell viability and plastid biogenesis. Proc. Natl. Acad. Sci. USA **105:** 3163–3168.

**Bartley, G.E., and Ishida, B.K.** (2003). Developmental gene regulation during tomato fruit ripening and in-vitro sepal morphogenesis. BMC Plant Biol. **3:** 4.

**Benjamini, Y., and Hochberg, Y.** (1995). Controlling the false discovery rate: A practical and powerful approach to multiple testing. J. R. Statist. Soc. **57:** 289–300.

**Bishop, G.J., Nomura, T., Yokota, T., Harrison, K., Noguchi, T., Fujioka, S., Takatsuto, S., Jones, J.D.G., and Kamiya, Y.** (1999). The tomato DWARF enzyme catalyses C-6 oxidation in brassinosteroid biosynthesis. Proc. Natl. Acad. Sci. USA **96:** 1761–1766.

**Blankemeyer, J.T., White, J.B., Stringer, B.K., and Friedman, M.** (1997). Effect of $\alpha$-tomatine and tomatidine on membrane potential of frog embryos and active transport of ions in frog skin. Food Chem. Toxicol. **35:** 639–646.

**Bouarab, K., Melton, R., Peart, J., Baulcombe, D., and Osbourn, A.** (2002). A saponin-detoxifying enzyme mediates suppression of plant defences. Nature **418:** 889–892.

**Bowles, D.** (2002). A multigene family of glycosyltransferases in a model plant, *Arabidopsis thaliana*. Biochem. Soc. Trans. **30:** 301–306.

**Bowles, D., Lim, E.K., Poppenberger, B., and Vaistij, F.E.** (2006). Glycosyltransferases of lipophilic small molecules. Annu. Rev. Plant Biol. **57:** 567–597.

**Carland, F.M., Fujioka, S., and Nelson, T.** (2010). The sterol methyltransferases SMT1, SMT2, and SMT3 influence Arabidopsis development through nonbrassinosteroid products. Plant Physiol. **153:** 741–756.

**Carland, F.M., Fujioka, S., Takatsuto, S., Yoshida, S., and Nelson, T.** (2002). The identification of CVP1 reveals a role for sterols in vascular patterning. Plant Cell **14:** 2045–2058.

**Cataldi, T.R.I., Lelario, F., and Bufo, S.A.** (2005). Analysis of tomato glycoalkaloids by liquid chromatography coupled with electrospray ionization tandem mass spectrometry. Rapid Commun. Mass Spectrom. **19:** 3103–3110.

**Chan, H.T.J., and Tam, S.Y.T.** (1985). Toxicity of $\alpha$-tomatine to larvae of the Mediterranean fruit fly (*Diptera*:*Tephritidae*). J. Econ. Entomol. **78:** 305–307.

**Chuartzman, S.G., Nevo, R., Shimoni, E., Charuvi, D., Kiss, V., Ohad, I., Brumfeld, V., and Reich, Z.** (2008). Thylakoid membrane remodeling during state transitions in *Arabidopsis*. Plant Cell **20:** 1029–1039.

**Eich, E.** (2008). *Solanaceae* and *Convolvulaceae* - Secondary Metabolites: Biosynthesis, Chemotaxonomy, Biological and Economic Significance: A Handbook. (Berlin: Springer).

**Expósito-Rodríguez, M., Borges, A.A., Borges-Pérez, A., and Pérez, J.A.** (2008). Selection of internal control genes for quantitative real-time RT-PCR studies during tomato development process. BMC Plant Biol. **8:** 131.

**Friedman, M.** (2002). Tomato glycoalkaloids: Role in the plant and in the diet. J. Agric. Food Chem. **50:** 5751–5780.

**Friedman, M., Roitman, J.N., and Kozukue, N.** (2003). Glycoalkaloid and calystegine contents of eight potato cultivars. J. Agric. Food Chem. **51:** 2964–2973.

**Fujiwara, Y., Takaki, A., Uehara, Y., Ikeda, T., Okawa, M., Yamauchi, K., Ono, M., Yoshimitsu, H., and Nohara, T.** (2004). Tomato steroidal alkaloid glycosides, esculeosides A and B, from ripe fruits. Tetrahedron **60:** 4915–4920.

**Gibly, A., Bonshtien, A., Balaji, V., Debbie, P., Martin, G.B., and Sessa, G.** (2004). Identification and expression profiling of tomato genes differentially regulated during a resistance response to *Xanthomonas campestris* pv. *vesicatoria.* Mol. Plant Microbe Interact. **17:** 1212–1222.

**Gouy, M., Guindon, S., and Gascuel, O.** (2010). SeaView version 4: A multiplatform graphical user interface for sequence alignment and phylogenetic tree building. Mol. Biol. Evol. **27:** 221–224.

**Guindon, S., and Gascuel, O.** (2003). A simple, fast, and accurate algorithm to estimate large phylogenies by maximum likelihood. Syst. Biol. **52:** 696–704.

**Gunther, C., Gonzalez, A., Reis, R.D., Gonzalez, G., Vazquez, A., Ferreira, F., and Moyna, P.** (1997). Effect of *Solanum* glycoalkaloids on potato afid, *Macrosiphum euphorbiae.* J. Chem. Ecol. **23:** 1651–1659.

**He, J.X., Fujioka, S., Li, T.C., Kang, S.G., Seto, H., Takatsuto, S., Yoshida, S., and Jang, J.C.** (2003). Sterols regulate development and gene expression in Arabidopsis. Plant Physiol. **131:** 1258–1269.

**Herner, R.C., and Sink, K.C.** (1973). Ethylene production and respiratory behavior of the *rin* tomato mutant. Plant Physiol. **52:** 38–42.

**Hoagland, R.E.** (2009). Toxicity of tomatine and tomatidine on weeds, crops and phytopathogenic fungi. Allelopathy J. **23:** 425–436.

**Hong, J.K., Choi, H.W., Hwang, I.S., Kim, D.S., Kim, N.H., Choi, S., Kim, Y.J., and Hwang, B.K.** (2008). Function of a novel GDSL-type pepper lipase gene, *CaGLIP1*, in disease susceptibility and abiotic stress tolerance. Planta **227:** 539–558.

**Iijima, Y., Fujiwara, Y., Tokita, T., Ikeda, T., Nohara, T., Aoki, K., and Shibata, D.** (2009). Involvement of ethylene in the accumulation of esculeoside A during fruit ripening of tomato (*Solanum lycopersicum*). J. Agric. Food Chem. **57:** 3247–3252.

**Iijima, Y., et al.** (2008). Metabolite annotations based on the integration of mass spectral information. Plant J. **54:** 949–962.

**Irizarry, R.A., Bolstad, B.M., Collin, F., Cope, L.M., Hobbs, B., and Speed, T.P.** (2003). Summaries of Affymetrix GeneChip probe level data. Nucleic Acids Res. **31:** e15.

**Itkin, M., Seybold, H., Breitel, D., Rogachev, I., Meir, S., and Aharoni, A.** (2009). TOMATO AGAMOUS-LIKE 1 is a component of the fruit ripening regulatory network. Plant J. **60:** 1081–1095.

**Ito, S., Eto, T., Tanaka, S., Yamauchi, N., Takahara, H., and Ikeda, T.** (2004). Tomatidine and lycotetraose, hydrolysis products of $\alpha$-tomatine by *Fusarium oxysporum* tomatinase, suppress induced defense responses in tomato cells. FEBS Lett. **571:** 31–34.

**Jang, C.S., Kim, J.Y., Haam, J.W., Lee, M.S., Kim, D.S., Li, Y.W., and Seo, Y.W.** (2003). Expressed sequence tags from a wheat-rye translocation line (2BS/2RL) infested by larvae of Hessian fly [*Mayetiola destructor* (Say)]. Plant Cell Rep. **22:** 150–158.

**Jones, J.B., Jones, J.P., Stall, R.E., and Zitter, T.A.** (1997). Compendium of Tomato Diseases. (St. Paul, MN: APS Press).

**Kalinowska, M., Zimowski, J., Paczkowski, C., and Wojciechowski, Z.A.** (2005). The formation of sugar chains in triterpenoid saponins and glycoalkaloids. Phytochem. Rev. **4:** 237–257.

**Karimi, M., Inzé, D., and Depicker, A.** (2002). GATEWAY vectors for Agrobacterium-mediated plant transformation. Trends Plant Sci. **7:** 193–195.

**Karlova, R., Rosin, F.M., Busscher-Lange, J., Parapunova, V., Do, P.T., Fernie, A.R., Fraser, P.D., Baxter, C., Angenent, G.C., and de Maagd, R.A.** (2011). Transcriptome and metabolite profiling show that APETALA2a is a major regulator of tomato fruit ripening. Plant Cell **23:** 923–941.

**Kaup, O., Gräfen, I., Zellermann, E.M., Eichenlaub, R., and Gartemann, K.H.** (2005). Identification of a tomatinase in the tomato-pathogenic actinomycete *Clavibacter michiganensis* subsp. *michiganensis* NCPPB382. Mol. Plant Microbe Interact. **18:** 1090–1098.

**Keukens, E.A., de Vrije, T., Fabrie, C.H., Demel, R.A., Jongen, W.M., and de Kruijff, B.** (1992). Dual specificity of sterol-mediated glycoalkaloid induced membrane disruption. Biochim. Biophys. Acta **1110:** 127–136.

**Keukens, E.A., de Vrije, T., van den Boom, C., de Waard, P., Plasman, H.H., Thiel, F., Chupin, V., Jongen, W.M., and de Kruijff, B.** (1995). Molecular basis of glycoalkaloid induced membrane disruption. Biochim. Biophys. Acta **1240:** 216–228.

**Ko, M.K., Jeon, W.B., Kim, K.S., Lee, H.H., Seo, H.H., Kim, Y.S., and Oh, B.J.** (2005). A *Colletotrichum gloeosporioides*-induced esterase gene of nonclimacteric pepper (*Capsicum annuum*) fruit during ripening plays a role in resistance against fungal infection. Plant Mol. Biol. **58:** 529–541.

**Kohara, A., Nakajima, C., Hashimoto, K., Ikenaga, T., Tanaka, H., Shoyama, Y., Yoshida, S., and Muranaka, T.** (2005). A novel glucosyltransferase involved in steroid saponin biosynthesis in *Solanum aculeatissimum.* Plant Mol. Biol. **57:** 225–239.

**Kozukue, N., Han, J.S., Lee, K.R., and Friedman, M.** (2004). Dehydrotomatine and $\alpha$-tomatine content in tomato fruits and vegetative plant tissues. J. Agric. Food Chem. **52:** 2079–2083.

**Kozukue, N., Yoon, K.S., Byun, G.I., Misoo, S., Levin, C.E., and Friedman, M.** (2008). Distribution of glycoalkaloids in potato tubers of 59 accessions of two wild and five cultivated *Solanum* species. J. Agric. Food Chem. **56:** 11920–11928.

**Krits, P., Fogelman, E., and Ginzberg, I.** (2007). Potato steroidal glycoalkaloid levels and the expression of key isoprenoid metabolic genes. Planta **227:** 143–150.

**Larkin, M.A., et al.** (2007). Clustal W and Clustal X version 2.0. Bioinformatics **23:** 2947–2948.

**Lineweaver, H., and Burk, D.** (1934). The determination of enzyme dissociation constants. J. Am. Chem. Soc. **56:** 658–666.

**Mackenzie, P.I., et al.** (1997). The UDP glycosyltransferase gene superfamily: Recommended nomenclature update based on evolutionary divergence. Pharmacogenetics **7:** 255–269.

**McCue, K.F., Allen, P.V., Shepherd, L.V., Blake, A., Maccree, M.M., Rockhold, D.R., Novy, R.G., Stewart, D., Davies, H.V., and Belknap, W.R.** (2007). Potato glycosterol rhamnosyltransferase, the terminal step in triose side-chain biosynthesis. Phytochemistry **68:** 327–334.

**McCue, K.F., Allen, P.V., Shepherd, L.V., Blake, A., Whitworth, J., Maccree, M.M., Rockhold, D.R., Stewart, D., Davies, H.V., and Belknap, W.R.** (2006). The primary in vivo steroidal alkaloid glucosyltransferase from potato. Phytochemistry **67:** 1590–1597.

**McCue, K.F., Shepherd, L.V.T., Allen, P.V., Maccree, M.M., Rockhold, D.R., Corsini, D.L., Davies, H.V., and Belknap, W.R.** (2005). Metabolic compensation of steroidal glycoalkaloid biosynthesis in transgenic potato tubers: using reverse genetics to confirm the *in vivo* enzyme function of a steroidal alkaloid galactosyltransferase. Plant Sci. **168:** 267–273.

**McKee, R.K.** (1959). Factors affecting the toxicity of solanine and related alkaloids to *Fusarium caeruleum*. J. Gen. Microbiol. **20:** 686–696.

**Meissner, R., Chague, V., Zhu, Q., Emmanuel, E., Elkind, Y., and Levy, A.A.** (2000). Technical advance: A high throughput system for transposon tagging and promoter trapping in tomato. Plant J. **22:** 265–274.

**Meissner, R., Jacobson, Y., Melamed, S., Levyatuv, S., Shalev, G., Ashri, A., Elkind, Y., and Levy, A.** (1997). A new model system for tomato genetics. Plant J. **12:** 1465–1472.

**Mintz-Oron, S., Mandel, T., Rogachev, I., Feldberg, L., Lotan, O., Yativ, M., Wang, Z., Jetter, R., Venger, I., Adato, A., and Aharoni, A.** (2008). Gene expression and metabolism in tomato fruit surface tissues. Plant Physiol. **147:** 823–851.

**Moco, S., Bino, R.J., Vorst, O., Verhoeven, H.A., de Groot, J., van Beek, T.A., Vervoort, J., and de Vos, C.H.** (2006). A liquid chromatography-mass spectrometry-based metabolome database for tomato. Plant Physiol. **141:** 1205–1218.

**Moco, S., Capanoglu, E., Tikunov, Y., Bino, R.J., Boyacioglu, D., Hall, R.D., Vervoort, J., and De Vos, R.C.** (2007). Tissue specialization at the metabolite level is perceived during the development of tomato fruit. J. Exp. Bot. **58:** 4131–4146.

**Moehs, C.P., Allen, P.V., Friedman, M., and Belknap, W.R.** (1997). Cloning and expression of solanidine UDP-glucose glucosyltransferase from potato. Plant J. **11:** 227–236.

**Morrissey, J.P., and Osbourn, A.E.** (1999). Fungal resistance to plant antibiotics as a mechanism of pathogenesis. Microbiol. Mol. Biol. Rev. **63:** 708–724.

**Murashige, T., and Skoog, F.** (1962). A revised medium for rapid growth and bio-assays with tobacco tissue cultures. Physiol. Plant. **15:** 473–497.

**Mylona, P., Owatworakit, A., Papadopoulou, K., Jenner, H., Qin, B., Findlay, K., Hill, L., Qi, X., Bakht, S., Melton, R., and Osbourn, A.** (2008). Sad3 and sad4 are required for saponin biosynthesis and root development in oat. Plant Cell **20:** 201–212.

**Naoumkina, M.A., Modolo, L.V., Huhman, D.V., Urbanczyk-Wochniak, E., Tang, Y., Sumner, L.W., and Dixon, R.A.** (2010). Genomic and coexpression analyses predict multiple genes involved in triterpene saponin biosynthesis in *Medicago truncatula*. Plant Cell **22:** 850–866.

**Oka, K., Okubo, A., Kodama, M., and Otani, H.** (2006). Detoxification of $\alpha$-tomatine by tomato pathogens *Alternaria alternata* tomato pathotype and *Corynespora cassiicola* and its role in infection. J. Gen. Plant Pathol. **72:** 152–158.

**Paquette, S., Møller, B.L., and Bak, S.** (2003). On the origin of family 1 plant glycosyltransferases. Phytochemistry **62:** 399–413.

**Pareja-Jaime, Y., Roncero, M.I., and Ruiz-Roldán, M.C.** (2008). Tomatinase from *Fusarium oxysporum* f. sp. *lycopersici* is required for full virulence on tomato plants. Mol. Plant Microbe Interact. **21:** 728–736.

**Pautot, V., Holzer, F.M., and Walling, L.L.** (1991). Differential expression of tomato proteinase inhibitor I and II genes during bacterial pathogen invasion and wounding. Mol. Plant Microbe Interact. **4:** 284–292.

**Rahman, A.-u., Choudhary, M.I., and Geoffrey, A.C.** (1998). Chemistry and biology of steroidal alkaloids. In The Alkaloids, G.A. Cordell, ed (San Diego, CA: Academic Press), pp. 61–108.

**Roddick, J.G.** (1976a). Response of tissues and organs of tomato to exogenous $\alpha$-tomatine. J. Exp. Bot. **27:** 341–346.

**Roddick, J.G.** (1976b). Intracellular distribution of the steroidal glycoalkaloid $\alpha$-tomatine in *Lycopersicon esculentum* fruit. Phytochemistry **15:** 475–477.

**Roddick, J.G.** (1977). Subcellular localization of steroidal glycoalkaloidsin vegetative organs of Lycopersicon esculentum and *Solanum tuberosum*. Phytochemistry **16:** 805–807.

**Rodrigo, I., Vera, P., Frank, R., and Conejero, V.** (1991). Identification of the viroid-induced tomato pathogenesis-related (PR) protein P23 as the thaumatin-like tomato protein NP24 associated with osmotic stress. Plant Mol. Biol. **16:** 931–934.

**Rose, J.K., Lee, H.H., and Bennett, A.B.** (1997). Expression of a divergent expansin gene is fruit-specific and ripening-regulated. Proc. Natl. Acad. Sci. USA **94:** 5955–5960.

**Ruuska, S.A., and Ohlrogge, J.B.** (2001). Protocol for small-scale RNA isolation and transcriptional profiling of developing Arabidopsis seeds. Biotechniques **31:** 752, 754, 756–758.

**Sandrock, R.W., and Vanetten, H.D.** (1998). Fungal sensitivity to and enzymatic degradation of the phytoanticipin $\alpha$-tomatine. Phytopathology **88:** 137–143.

**Schaeffer, A., Bronner, R., Benveniste, P., and Schaller, H.** (2001). The ratio of campesterol to sitosterol that modulates growth in Arabidopsis is controlled by STEROL METHYLTRANSFERASE 2;1. Plant J. **25:** 605–615.

**Shakya, R., and Navarre, D.A.** (2008). LC-MS analysis of solanidane glycoalkaloid diversity among tubers of four wild potato species and three cultivars (*Solanum tuberosum*). J. Agric. Food Chem. **56:** 6949–6958.

**Simons, V., Morrissey, J.P., Latijnhouwers, M., Csukai, M., Cleaver, A., Yarrow, C., and Osbourn, A.** (2006). Dual effects of plant steroidal alkaloids on *Saccharomyces cerevisiae.* Antimicrob. Agents Chemother. **50:** 2732–2740.

**Steel, C.C., and Drysdale, R.B.** (1988). Electrolyte leakage from plant and fungal tissues and disruption of liposome membranes by $\alpha$-tomatine. Phytochemistry **27:** 1025–1030.

**Tamir-Ariel, D., Navon, N., and Burdman, S.** (2007). Identification of *Xanthomonas campestris* pv. *vesicatoria* genes induced in its interaction with tomato. J. Bacteriol. **189:** 6359–6371.

**Thompson, A.J., Tor, M., Barry, C.S., Vrebalov, J., Orfila, C., Jarvis, M.C., Giovannoni, J.J., Grierson, D., and Seymour, G.B.** (1999). Molecular and genetic characterization of a novel pleiotropic tomato-ripening mutant. Plant Physiol. **120:** 383–390.

**Tu, J.C.** (1985). An improved Mathur's medium for growth, sporulation, and germination of spores of *Colletotrichum lindemuthianum.* Microbio. **44:** 87–93.

**Ueguchi-Tanaka, M., Ashikari, M., Nakajima, M., Itoh, H., Katoh, E., Kobayashi, M., Chow, T.Y., Hsing, Y.I., Kitano, H., Yamaguchi, I., and Matsuoka, M.** (2005). *GIBBERELLIN INSENSITIVE DWARF1* encodes a soluble receptor for gibberellin. Nature **437:** 693–698.

**Vera, P., Tornero, P., and Conejero, V.** (1993). Cloning and expression analysis of a viroid-induced peroxidase from tomato plants. Mol. Plant Microbe Interact. **6:** 790–794.

**Verwoerd, T.C., Dekker, B.M., and Hoekema, A.** (1989). A small-scale procedure for the rapid isolation of plant RNAs. Nucleic Acids Res. **17:** 2362.

**Yamanaka, T., Vincken, J.P., de Waard, P., Sanders, M., Takada, N., and Gruppen, H.** (2008). Isolation, characterization, and surfactant properties of the major triterpenoid glycosides from unripe tomato fruits. J. Agric. Food Chem. **56:** 11432–11440.

**Yamanaka, T., Vincken, J.P., Zuilhof, H., Legger, A., Takada, N., and Gruppen, H.** (2009). C22 isomerization in $\alpha$-tomatine-to-esculeoside A conversion during tomato ripening is driven by C27 hydroxylation of triterpenoidal skeleton. J. Agric. Food Chem. **57:** 3786–3791.

**Yokotani, N., Nakano, R., Imanishi, S., Nagata, M., Inaba, A., and Kubo, Y.** (2009). Ripening-associated ethylene biosynthesis in tomato fruit is autocatalytically and developmentally regulated. J. Exp. Bot. **60:** 3433–3442.

**Zimowski, J.** (1998). Specificity and properties of UDP-galactose: tomatidine galactosyltransferase from tomato leaves. Plant Sci. **136:** 139–148.